AD-A222 027

90 05 25 140

(2)

REPORT DOCUMENTATION PAGE

Form Approved
OMB No. 0704-0188

1. AGENCY USE ONLY (Leave blank)	2. REPORT DATE	3. REPORT TYPE AND DATES COVERED
	February 28, 1990	Annual Report 89-90

4. TITLE AND SUBTITLE
Micromechanics of Interfaces in High Temperature Ceramics

5. FUNDING NUMBERS
G-AFOSR-89-0269
61102F
2302/B2

6. AUTHOR(S)
T. Mura, J. O. Brittain and K. Faber

7. PERFORMING ORGANIZATION NAME(S) AND ADDRESS(ES)
Northwestern University
Center for Quality Engineering and Failure Prevention
Evanston, IL 60208

8. PERFORMING ORGANIZATION REPORT NUMBER
0650-350-R402
A.R. -1

9. SPONSORING/MONITORING AGENCY NAME(S) AND ADDRESS(ES)
Dr. Liselotte J. Schioler
Colonel George K. Haritos
Air Force Office of Scientific Research
Bolling Air Force Base
Washington, D.C. 20332

10. SPONSORING/MONITORING AGENCY REPORT NUMBER
AFOSR-TR- 90-0571

11. SUPPLEMENTARY NOTES

12a. DISTRIBUTION/AVAILABILITY STATEMENT
Unlimited

12b. DISTRIBUTION CODE

13. ABSTRACT (Maximum 200 words)

Results of the initial phase of a program to investigate the micromechanics of interfaces are summarized. Model experiments have been devised and implemented to follow crack propagation in a fiber reinforced transparent matrix by visual observations and electrical resistance of the fiber. In addition, pull-out test on the same composites have been carried out with several matrix-fiber interface modifications. Some success has been achieved in separating debonding and frictional components at the interface.

We also report on the very early stage of experiments that have been initiated to study the in-situ debonding behavior during pull-out in a ceramic composite by utilizing a photo-elastic technique.

14. SUBJECT TERMS	15. NUMBER OF PAGES
Ceramic, acrylic, steel wire, fracture, debonding friction constant, photoelastic, mechanical behavior, composite materials	
	16. PRICE CODE

17. SECURITY CLASSIFICATION OF REPORT	18. SECURITY CLASSIFICATION OF THIS PAGE	19. SECURITY CLASSIFICATION OF ABSTRACT	20. LIMITATION OF ABSTRACT
unclassified	unclassified	unclassified (50)	unlimited

First Annual Report on

MICROMECHANICS OF INTERFACES IN HIGH TEMPERATURE CERAMICS

Authors: Professors Toshio Mura
John O. Brittain
Katherine Faber

Overall Objective:

Microstructural variables that allow toughness optimization will be established from analytical and experimental perspectives. The role of interfaces in terms of the debonding and the frictional sliding components contributed to resistance to crack propagation in ceramic matrix composites is the focus of both the experimental and theoretical phase of this research effort.

Status of Reserch Effort:

(1) We have undertaken model experiments on crack propagation in a fiber reinforced material. Crack propagation in acrylic-matrix-steel wire fiber composites have been monitored utilizing a double cantilever beam specimen configuration. The propagation of the crack was initiated by a wedge attached to either a micrometer or the moveable cross head of a 1125 Instron Testing Machine. With either of these modes of controlling the advancement of the wedge, the crack propagation was observed either visually or with the aid of an optical microscope. The visual observations of the resistance of the steel fiber to the propagation of the crack was complimented by the measurement of the change in the electrical resistance of the steel wire as the crack approached and passed the fiber. The electrical resistance measurements were made simultaneously with the force required to drive the crack. Greater details of this effort are described in the report appended as Appendix A.

In addition to the crack propagation studies, a series of pull-out tests have been made with the objective of trying to separate the debonding and frictional force contribution to crack propagation resistance. These experiments were also conducted on the acrylic-steel fiber composite so as to take advantage of the transparency of the matrix and the ease of fabricating the composites. The influence of interfacial bonding or lack of bonding was investigated via treatment of the surface of the steel fiber prior to fabrication of the fiber. At this time it appears that we can separate the individual contributions of the interface to toughness and can obtain a measure of the frictional force that acts during pull-out of a steel fiber in an acrylic matrix. Again greater details on the pull-out experiments can be found in the report appended as Appendix B.

Future effort based upon the acrylic-steel fiber composite will be directed towards monitoring the resistance to crack propagation in multi fiber-acrylic matrix components. An effort has also been initiated to determine if displacement of the fiber relative to the matrix can be

quantitatively determined in order to assist in the separation of the debonding and frictional phenomena during fiber-pull-out in opaque composites. Preparation of LAS matrix composites that are transparent is also to be undertaken.

The third effort currently in progress is concerned with a study of in-situ debonding behavior during fiber pull-out in a ceramic composite by utilizing a photoelastic technique. The objective of this research is to resolve the ambiguities in interpreting the load-displacement curves of single-fiber pull-out tests. The samples currently under study consist of ceramic rods embedded in a transparent glass matrix. The effect of interfacial cohesion will be effected by carbon coating the ceramic rod to various thickness. This surface treatment will influence the chemical bond between the rod and the matrix. In addition the surface treatment will serve to relieve or minimize the thermal mismatch. At this time these experiments are in the preliminary stage with the major attention directed towards the fabrication of suitable composites. Additional details of this phase of the research are to be found in Appendix C.

Professional Personnel Associated with the Research Effort:

1. Toshio Mura, Professor, Department of Civil Engineering
2. Katherine Faber, Associate Professor, Department of Materials Science and Engineering
3. John O. Brittain, Professor Emeritus, Department of Materials Science and Engineering

Research Personnel

4. Dr. Eizo Yoshitake, Post-Doctoral Fellow, Department of Materials Science and Engineering
5. Dr. Hongda Cai, Post-Doctoral Fellow, Department of Materials Science and Engineering
6. Daniel Mumm, Research Assistant, Department of Material Science and Engineering
7. Yoshio Makita, Research Assistant, Department of Materials Science and Engineering
8. Wen-Bin Tsai, Research Assistant, Department of Civil Engineering

Papers

The reports included in Apppendices A and B will be prepared for submission for publication in the near future.

Appendix A

DIRECT AND INDIRECT OBSERVATIONS OF CRACK PROPAGATION IN FIBER REINFORCED COMPOSITE MATERIALS

by

Eizo Yoshitake, Yoshio Makita, Toshio Mura and John O. Brittain

Abstract

This paper reports the results of model experiments on crack propagation in a fiber reinforced composite material. Crack propagation in fiber reinforced composite materials (steel wire and acrylic matrix) were continuously observed by an optical microscope. The steel wire has good resistance to crack propagation and the surface condition of the wire was controlled. The crack stops propagating when it reaches the wire. Then it separates into two partial cracks and they propagate around the wire. After passing past the wire, they unite and propagate as one crack. Crack propagation around the wire was investigated by observing the electrical resistance of the wire during crack propagation. The results of the resistance measurements suggest that when the crack propagates to the wire the crack angle starts to increase without opening at the wire. When the crack reaches the wire it stops propagating until the crack suddenly opens at the wire with further propagation.

Introduction

It is very important to understand the crack behavior around a fiber in composite materials in order to establish a theory of crack propagation [1,2]. Since the crack behavior at a fiber will depend upon the boundary conditions, crack propagation, with fibers having various boundary

treatments, was monitored by an optical microscope. Our main purpose of this experiment was to determine how a crack interacts with a fiber in a composite material.

Experiment Procedures

The fiber reinforced composite materials were made by hot-pressing two acrylic sheets (Acrylite FF by CYRO Industries) and a steel wire (music wire) which was placed between the two acrylic sheets. The composition of the wire was C 0.75-0.95, Mn 0.60 max, Si 0.28 max, S 0.030 max, P 0.024 max and Fe balance. The temperature of the hot-press was about 155^{o}C and the pressure (about 600 psi) was slowly applied to the sheets and wire. Then the material was slowly cooled to room temperature. The acrylic sheet was selected for the matrix material because of its transparency, low toughness and ease of fabrication. The music wire was selected for its high strength, relative toughness and the ease of achieving surface modifications. The transparency of the acrylic sheet-steel wire composite (A-S composite) made possible the observations of crack propagation.

The surface conditions of wires were changed by application of grease, polishing the surface with emery paper and oxidation of the surface. The test pieces were cut from the hot-pressed composite with a slow speed saw into sizes of 10x20x3 mm for pull-out test and 20x20x3 mm for crack propagation observation in a double cantilever beam (DCB) specimen.

The pull-out tests were performed using an Instron 1125 Machine with a cross-head speed of 0.5 mm/min to determine the bonding and frictional forces. The test piece and the test procedure are shown in Fig. 1. The

specimens were supported at the shoulders of the top part and the wire was gripped by a pair of stainless steel plates.

Because the double cantilever beam (DCB) specimen configuration results in relatively steady-state crack propagation [3-5], it was used for crack propagation observations. As shown in Fig. 2, strain was applied to the specimen by advancing an 11° wedge which is attached to a micrometer to control the displacement of the wedge. The whole system was placed under an optical microscope to observe crack propagation.

As shown in Fig. 3, the electrical resistance of the wire was measured with a modified DCB specimen with application of constant motion of a razor blade by the Instron Machine to obtain the slower crack speed. A constant current of 50 mA was supplied by a Keithley 227 Current Source and the voltage drop was measured by Keithley 180 Digital Nanovolt-meter which was connected to an X-t recorder.

Results and Discussion

1. Pull-Out Tests.

The effect of surface condition on bonding strength and friction force was examined by means of wire pull-out tests of the A-S composites. In Fig. 4, the peak force to pull-out the wire from the A-S composite is plotted as a function of the displacement of the cross-head. The slope of the initial (dashed line) linear portion of each curve are almost the same, which is expected to correspond to the elastic constant of the wire. A maximum in force was usually observed at an early stage in the pull-out test. The largest peak force was obtained with the wire polished with 240 grit, the second was with the wire polished with 400 grit emery paper, the third was

with the "as-received and cleaned" wire and the smallest force was with the wires with a thin layer of apiezon vacuum grease and Si-vacuum grease. The largest force can be considered as the force required to initiate pull-out of the wire. Therefore, the composite with the largest force possessed the largest bonding strength and/or friction force. As expected, the bonding strength and/or friction force decreased with the application of grease, but was increased by polishing and oxidation. The details of the experiments and analysis of the pull-out tests are described in detail elsewhere [6].

2. Observations of Crack Propagation.

Crack propagation can be controlled by step by step advance of the wedge, that is, by a micrometer. Fig. 5 illustrates schematically the change of crack shape as it is restrained by the wire. First, a crack moves towards the wire with a flat tip (Fig. 5a) and reaches to the wire (Fig. 5b). Then, the crack splits into two coplanar branches that advance but the center part of the crack remains stopped by the wire (Fig. 5c). The branches of the crack propagate past the wire and finally coalesce as one crack which then moved forward (Fig. 5d). This was the common behavior of crack propagation in the A-S composite materials. An example of the situation depicted in Fig. 5c is shown in Fig. 6, where it is clearly seen that the two ends of a crack have moved around the wire. Observations on the interaction of a crack front and inclusions have been previously reported [7,8]. Our observations are in agreement with the bowing of a crack front between inclusions.

The resistance to crack propagation comes from the bonding strength and frictional force between the matrix and the fiber. Therefore, the effect of bonding strength and frictional force was investigated by changing the surface conditions of the wire. Figs. 7-9 show a series of micrographs of crack propagations for different surface conditions. Fig. 7 shows the crack propagation observed in an A-S composite whose wire was coated with a thin layer of Si grease before hot-pressing. It is expected that the application of Si grease on the wire reduces the bonding force and frictional force. The crack reaches the wire with a tip (Fig. 7a) perpendicular to the wire, a small amount of bowing around the wire occurs in a short time (too fast to take a micrograph). The two branches of the crack were united as one planar crack (Fig. 7b). Fig. 8 shows the crack propagation of an A-S composite with a wire as-received. An increase in the bonding strength and frictional force are expected for this A-S composite. After reaching the wire (Fig. 8a), the center part of the crack was stopped by the wire (Fig. 8b), but the crack separates into the two coplanar branches that move around the wire. The length of the branches prior to coalescence (Marked as "d" in the figure) was longer than that in Fig. 6. After that, the two parts of the crack were united and moved forward (Fig. 8c). Fig. 9 shows the crack propagation of an A-S composite with an oxidized wire. The results of the pull-out tests indicated that a large bonding strength and frictional force are expected for this composite. The crack hits the wire (Fig. 9a) and the two branches of the crack propagated around the wire (Fig. 9b). The length of the crack branches are longer than those observed in Figs. 7 and 8. After the two parts were united the crack continued to propagate (Fig. 9c). Similar crack propagation behavior was observed in an A-S composite with a

wire polished with 400 grid emery paper. It is concluded from the results above that the larger the bonding strength and/or frictional force, the longer the branches of cracks propagate, which means that a fiber with large bonding strength and/or frictional force will cause a greater resistance to the crack propagation in the composite materials. The degree of the resistance can be determined from the length of the two branches of the cracks prior to coalescence.

3. Electrical Resistance of Wire.

It is very difficult to observe the behavior of a crack tip in detail with an optical microscope. While we tried, we have not yet succeeded. Therefore, we decided to measure the electrical resistance of the wire to detect strain changes at the wire indirectly. As shown in Fig. 3, the electrical resistance was measured during the crack propagation in the DCB specimens. Fig. 10 shows the load and the voltage changes plotted as a function of cross-head displacement (CHD). The voltage was relatively constant at the beginning (Stage 1), where no crack propagation was observed. The resistance started to increase slightly when the load reached the initial maximum load, where the crack also started to propagate, and simultaneously the load decreased (Stage 2). The electrical resistance increased linearly with CHD while the load decreases and the crack moves toward the wire (Stage 3). After the crack reached the wire, the slope of the electrical resistance vs CHD plot increased. When the crack branched around the wire the load increased (Stage 4) and a sudden increase in resistance was observed when the two branches of the crack were united,

i.e., (Stage 5), the wire was still intact, as observed in previous crack propagation studies [9, 10].

At the beginning, when there was little or no strain on the wire, the resistance was constant (Stage 1). The linear increase in voltage at Stage 3 corresponds to the linear increase in strain on the wire, which suggests that the crack was propagating steadily. When the crack reached the wire, two types of crack behavior occurred, Fig. 11; Type A, the crack passes branched around the wire without changing the crack angle (Fig. 11a) and, Type B, the crack was pinned (an increase in the crack angle was required before branching occurred (Fig. 11b). If Type A propagation occurs, the increase of voltage in Stage 3 should not appear and the crack should propagate without any hesitation at the wire. If Type B propagation occurs, the increase can be explained as a result of the crack opening. The sudden increase in resistance is obviously caused by the sudden creation of a gap at the wire, which resulted in a large strain on the wire. Therefore, the crack propagation in A-S composite is determined to be Type B, that is, the crack opens before propagating past the wire.

Conclusions

With the composite materials and configuration used in the work:

(1) The bonding strength and/or frictional force can be controlled by the surface conditions of the wire; application of grease, oxidation and polishing.

(2) A crack in A-S composite stops at the wire, branches around it and branches are united when they passed some distance beyond the wire. The length of the branches was found to be a function of the interfacial bonding.

(3) From the resistance measurement, it was determined that a crack in the composite opens (increase in crack angle) before passing around the wire.

References

1. D. B. Marshall and A. G. Evans, "Failure Mechanisms in Ceramic-Fiber/Ceramic-Matrix Composites", Jnl. Am. Ceramic Soc. 68 (1985), 225.

2. D. B. Marshall, B. N. Cox and A. G. Evans, "The Mechanics of Matrix Cracking in Brittle Matrix Fiber Composites", Acta Met. 33 (1983), 2013.

3. R. G. Hoagland, A. R. Rosenfield and G. T. Hahn, "Mechanisms of Fast Fracture and Arrest in Steel", Met. Trans. 3 (1972), p. 123.

4. G. T. Hahn, R. G. Hoagland, A. R. Rosenfield and R. Sejnoha, "Rapid Crack Propagation in a High Strength Steel", Mat. Trans. 5, (1974), p. 475.

5. G. R. Hahn, R. G. Hoagland, M. F. Kanninen and A. R. Rosenfield, "A Preliminary Study of Fast Fracture and Arrest in the DCB Test Specimen", in "Proceedings of an International Conference on Dynamic Crack Propagation", ed. by G. C. Sih, (July 10-12, 1972) Noordhoff International Publishing.

6. E. Yodhitake, Y. Makita, T. Mura and J. O. Brittain, to be published.

7. F. F. Lange, "The Interaction of a Crack Front with a Second Phase Dispersion", Phil. Mag. 22 (1970), 983.

8. D. J. Green, P. N. Nicholson and J. D. Embury, "Fracture of a Brittle Particulate Composite", Jnl. Mat. Sci. 14 (1979), 1413.

9. J. Bowling and G. W. groves, J. Mater. Sci. 14, (1979), 443.

10. T. W. Coyle, E. R. Fuller, Jr., P. Swanson, T. Palamedes, Ceram. Eng. Sci. Proc. 8 (1989), 630.

Figure Captions

Fig. 1. Illustration of pull-out test.

Fig. 2. Illustration of crack propagation observation with DCB specimen.

Fig. 3. Illustration of electrical resistance measurement with DCB specimen.

Fig. 4. Peak load displacement plots of pull-out tests of A-S composites with a) ■ = wire polished with 240 grit, b) □ = wire polished with 400 grit, c) △ = as-received wire, d) ● = apiezon vacuum greased wire, and e) ○ = Si-vacuum greased wire.

Fig. 5. Illustration of crack branching as it propagated around the wire: a) approaching to the wire; b) hitting the wire; c) branching around the wire and; d) coalescence of the branches.

Fig. 6. Example of crack propagation branching as observed in an "A-S" composite with an as-received wire.

Fig. 7. Crack propagation of A-S composite with a wire Si grease coated; a) before hitting the wire and b) after passing beyond it.

Fig. 8. Crack propagation of A-S composite with an as-received wire; a) before hitting the wire, b) branching around it and c) after passing it.

Fig. 9. Crack propagation of A-S composite with an oxidized wire: a) before hitting the wire; b) branching around it and; c) after passing the wire.

Fig. 10. Load-displacement curve and voltage change of DCB A-S composite.

Fig. 11. Two types of crack tip behaviors at the wire; a) without change in geometry and b) with an increase in the crack angle before branching.

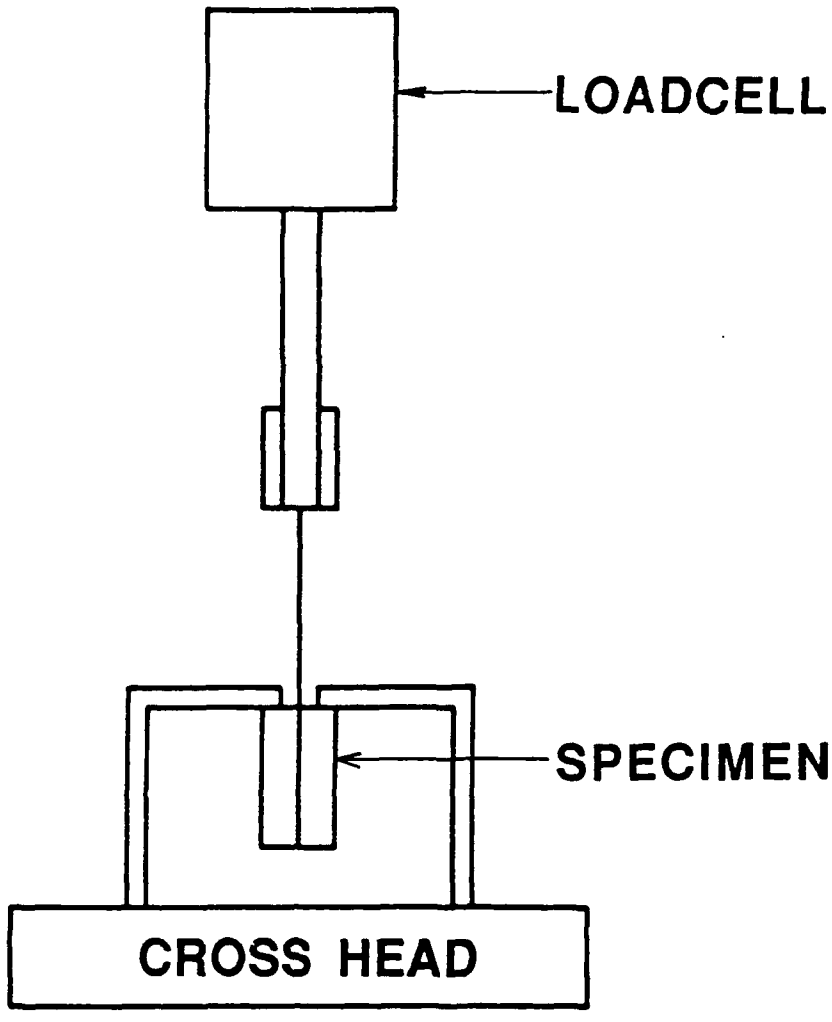

Fig 1

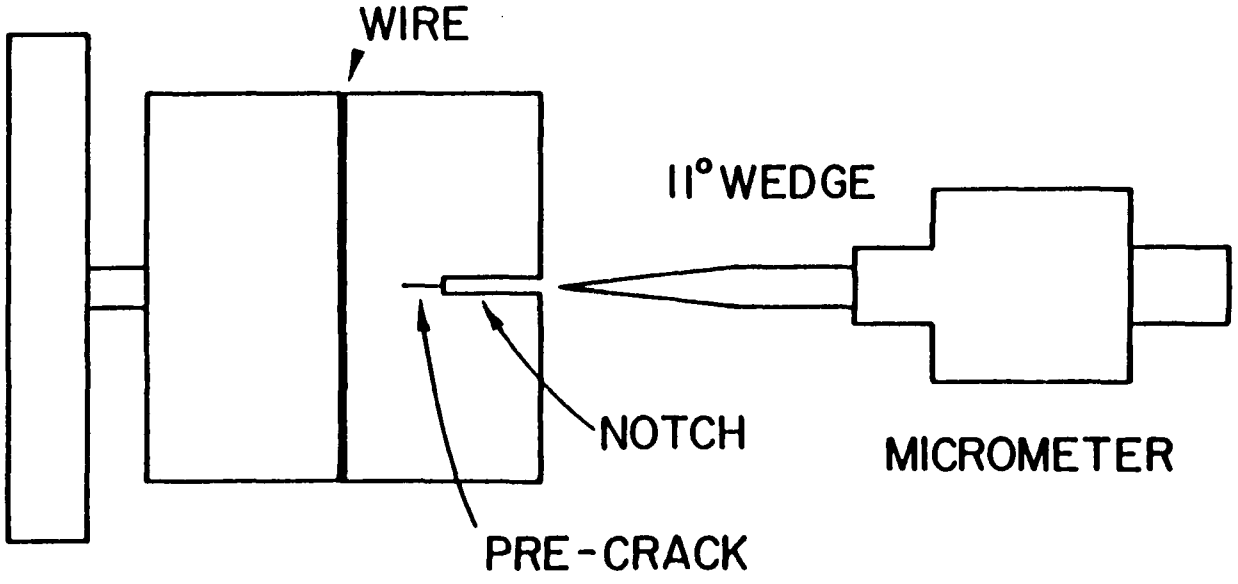
WIRE
11° WEDGE
NOTCH
MICROMETER
PRE-CRACK

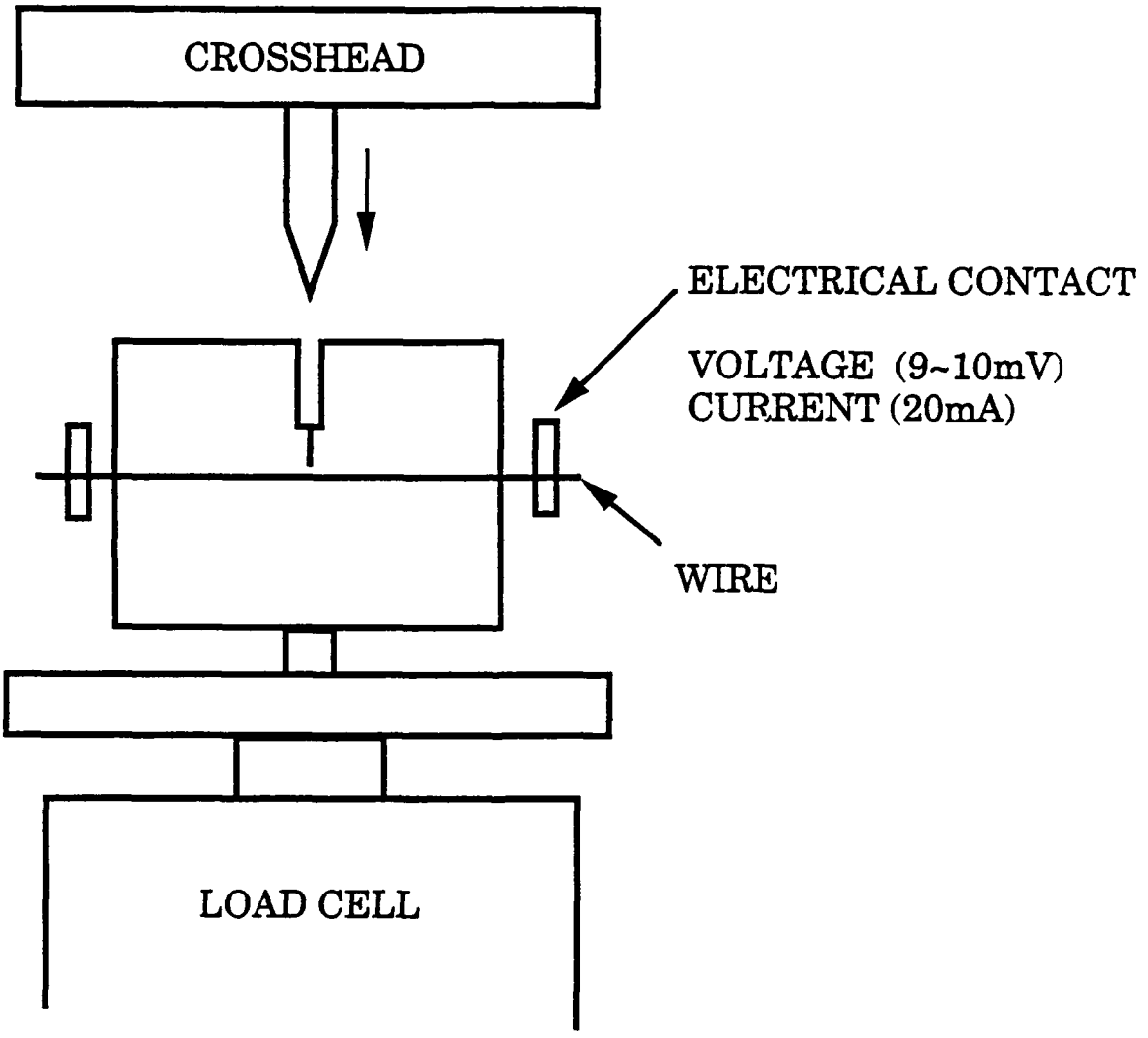
CROSSHEAD
ELECTRICAL CONTACT
VOLTAGE (9~10mV)
CURRENT (20mA)
WIRE
LOAD CELL

Fig 3

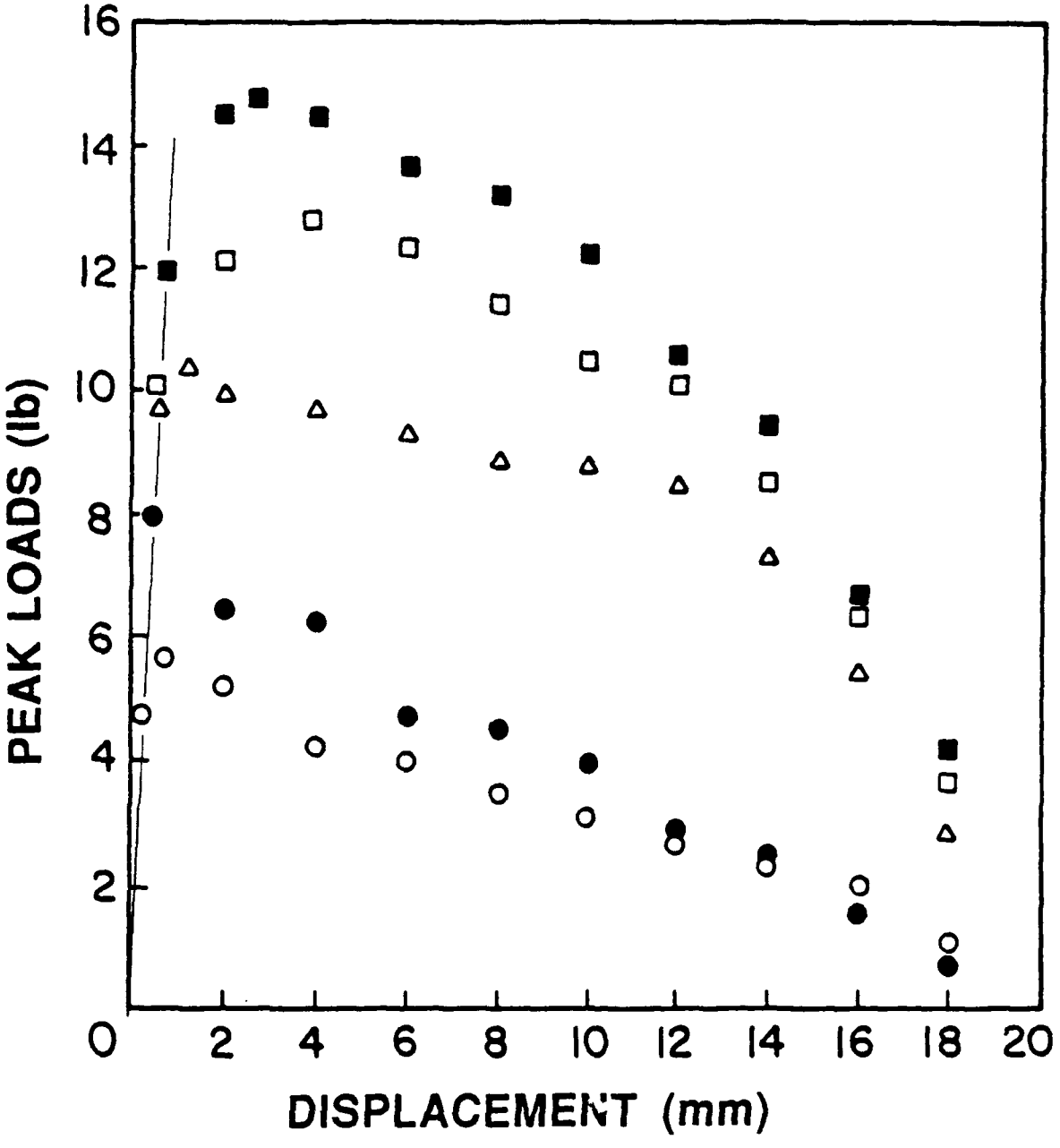
PEAK LOADS (lb)
16
14
12
10
8
6
4
2
0
2
4
6
8
10
12
14
16
18
20
DISPLACEMENT (mm)

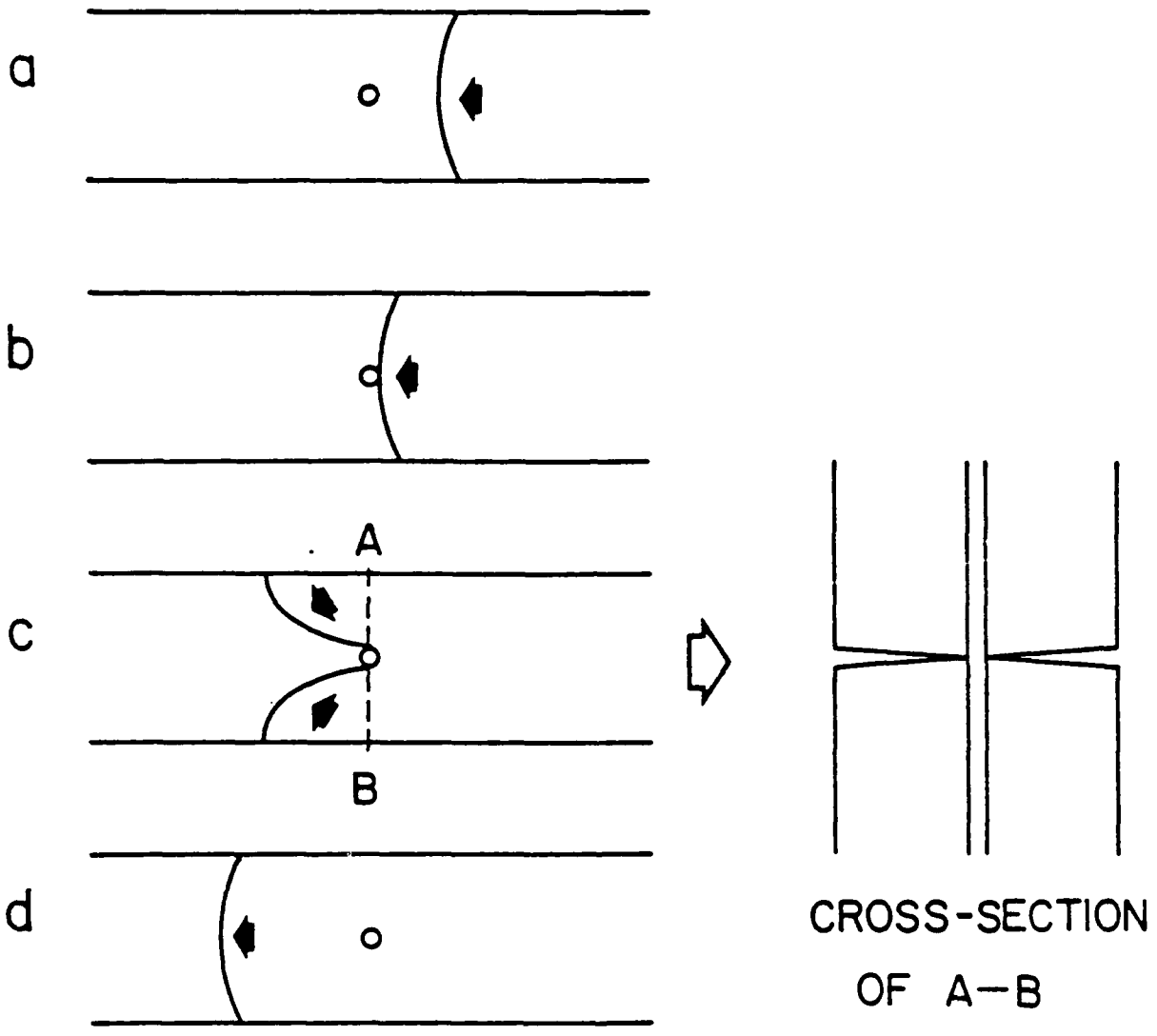

Fig 2

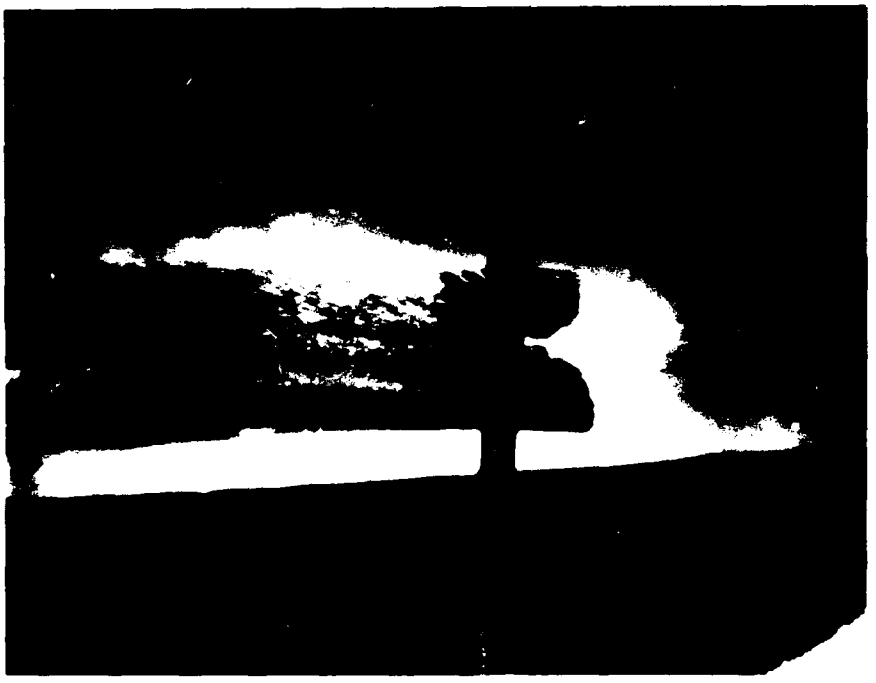

Fig. 6

(a)

(b)

Fig 2

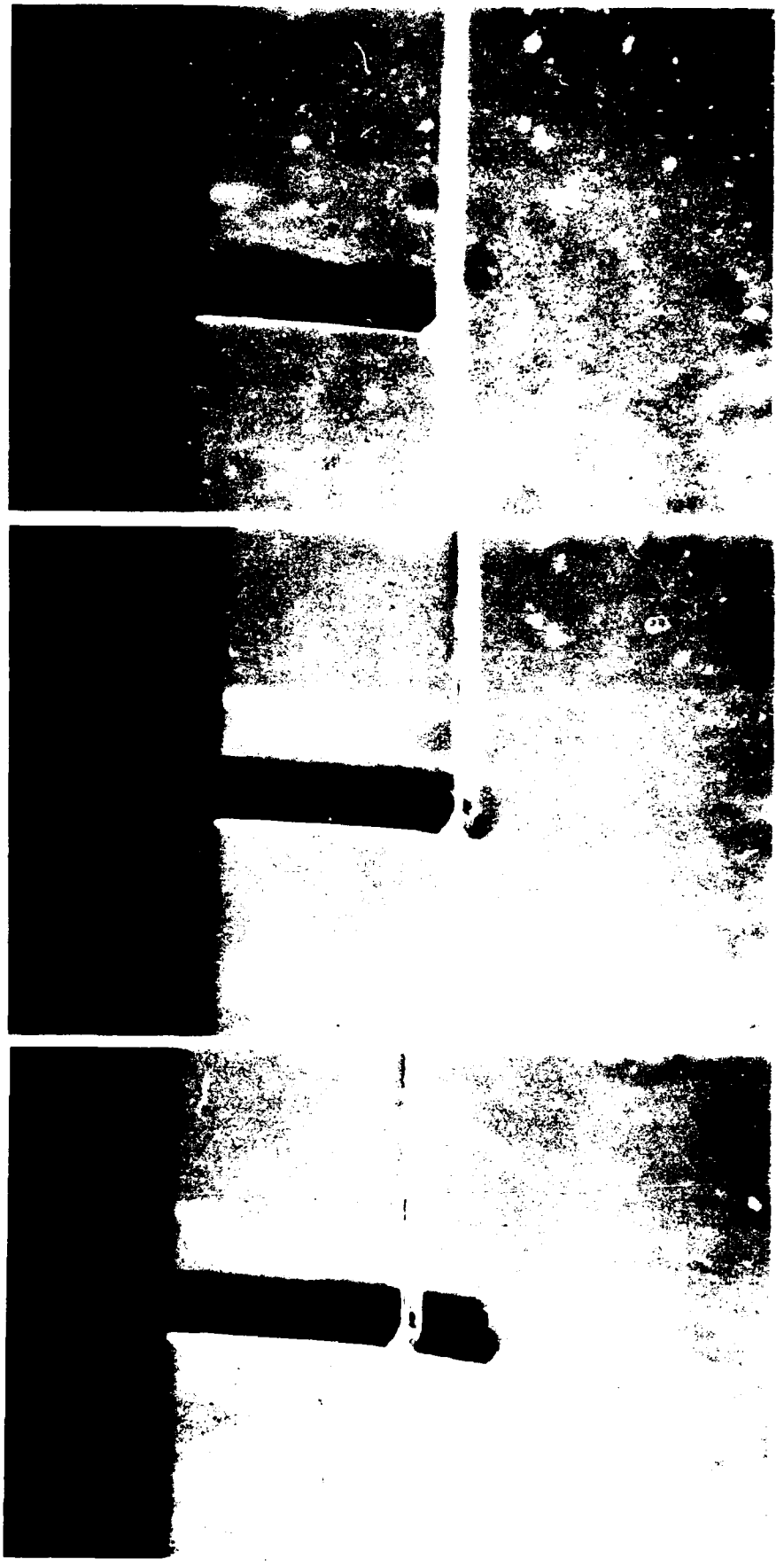

(a)

(b)

(c)

Fig. 8

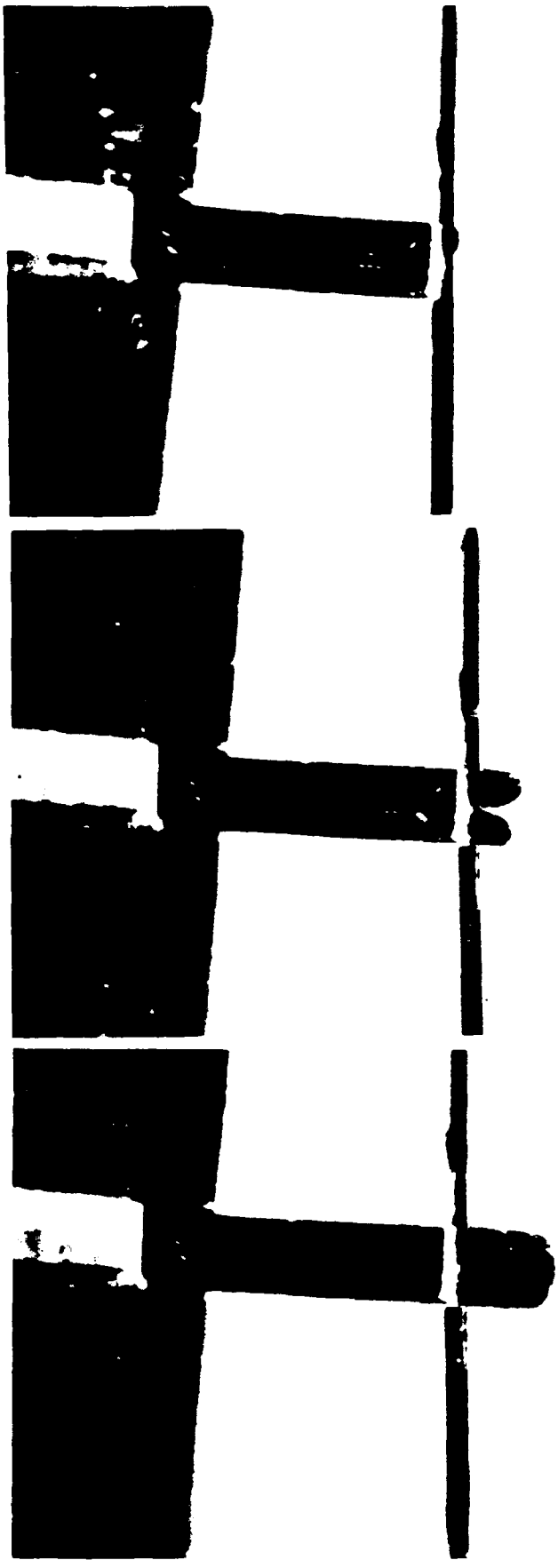

(a)

(b)

(c)

Fig 9

CRACK, LOAD AND RESISTANCE

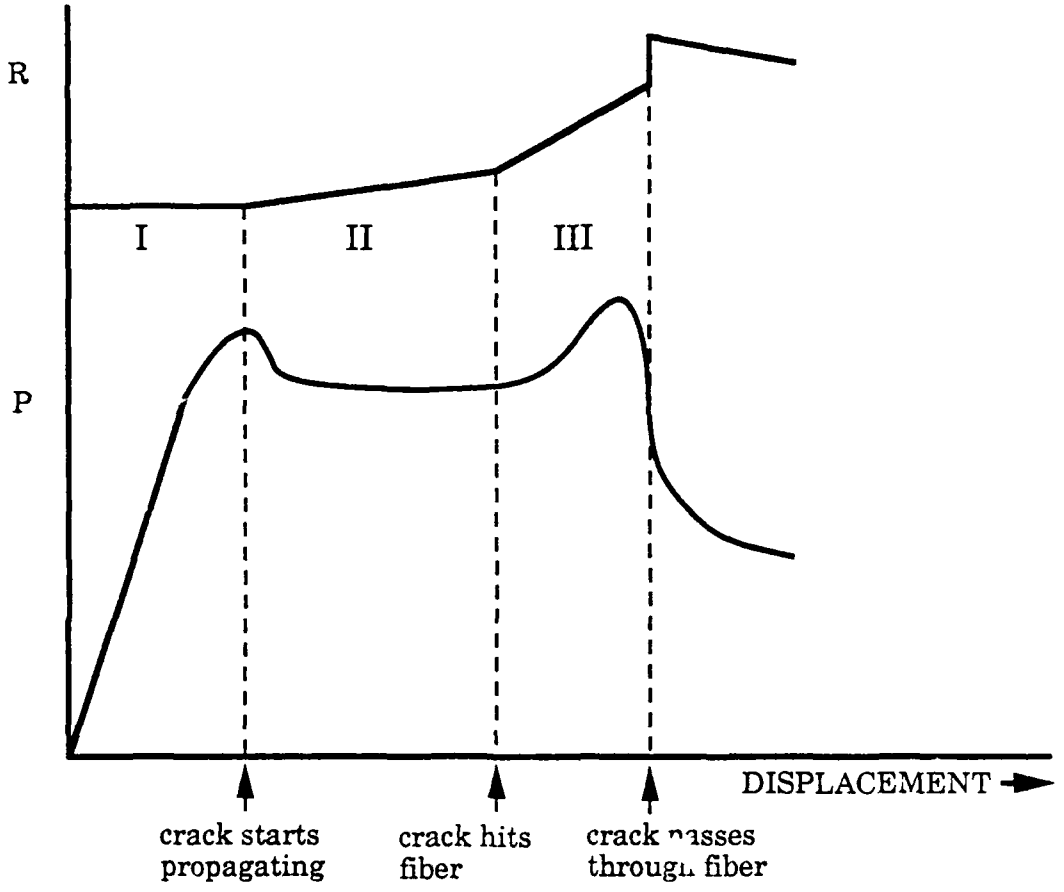

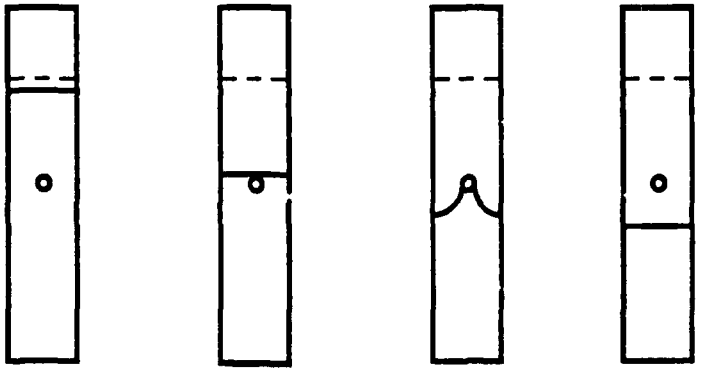

Fig 16

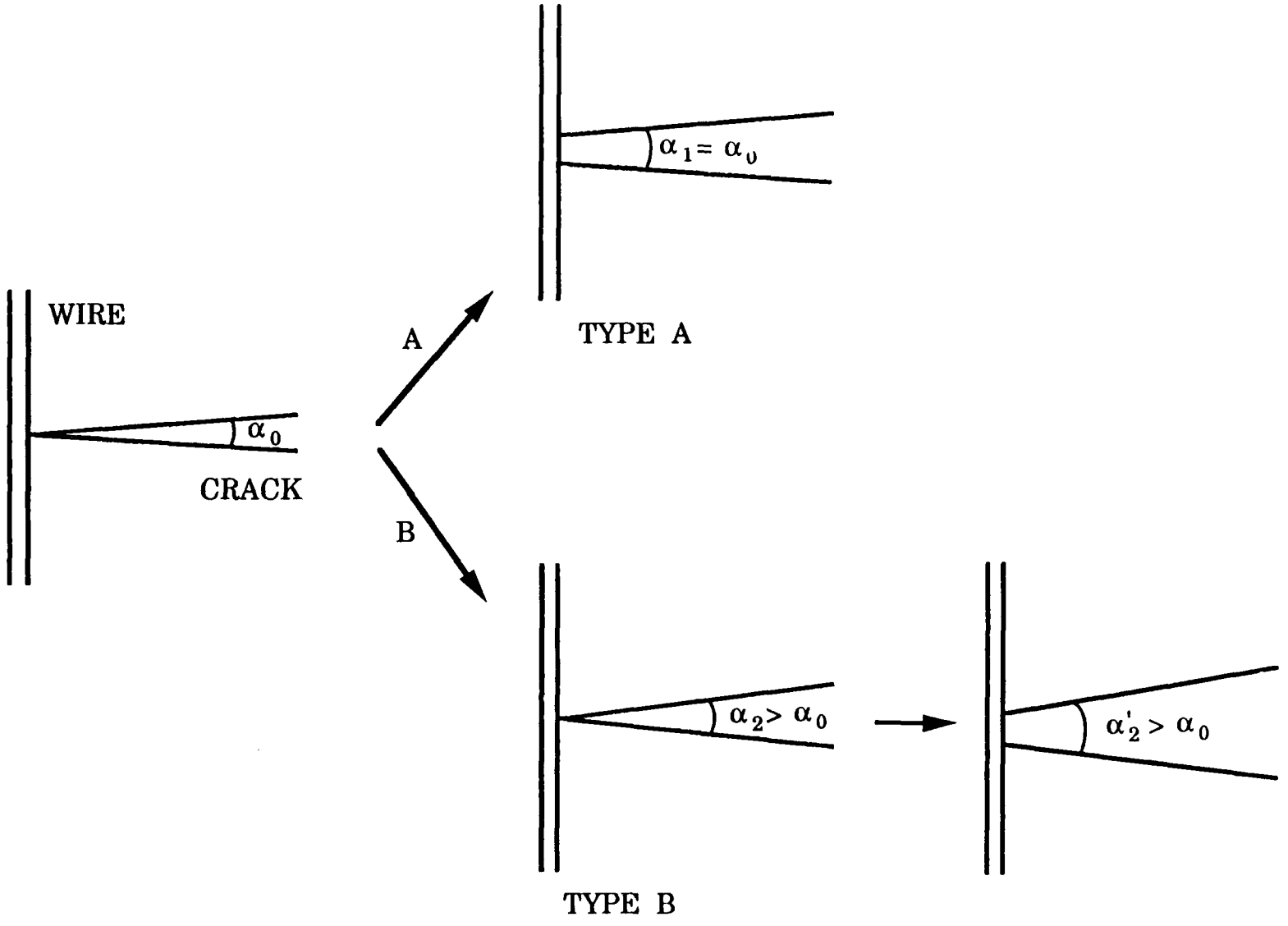
WIRE
α_0
CRACK
A
B
$\alpha_1 = \alpha_0$
TYPE A
$\alpha_2 > \alpha_0$
$\alpha'_2 > \alpha_0$
TYPE B

Appendix B

PULL-OUT TESTS OF FIBER COMPOSITES - - ANALYSIS OF BONDING STRENGTH AND FRICTIONAL FORCE

Ezio Yoshitake, Yoshio Makita, Wen-Bin Tsai,
Toshio Mura and John O. Brittain

Abstract

From a number of pull-out tests of acrylic-steel wire composites, the debonding and sliding behaviors are discussed in this paper. The "stick-slip" type sliding between the fiber and matrix was observed in this composite. The bonding strength and frictional force were dependent on the surface condition of the wire. Application of a thin layer of Si grease on the wire reduced the bonding strength and frictional force, while polishing of the wire with emery paper resulted in larger values. A partial debonding process was observed in long specimens and in specimens with polished wires. The magnitude of the load drops in the "stick-slip" phenomenon was reduced or not observed in specimen tested at high speeds. The experimental results are discussed in terms of a friction constant, bonding strength, stress and strain distribution and sliding speed. One of the main conclusions is that the "stick-slip" behavior may be a common process for the sliding of fibers to other composites if they are tested at sufficiently slow speed.

Introduction

Since the bonding strength and the frictional force are important factors that influence the toughness of the composites [1], it is very important to understand the debonding and sliding behavior between a fiber and a matrix in composite material. A pull-out test is one of the popular methods to study the sliding of a fiber in composite materials. Since it is

desirable to observe the debonding and sliding, acrylic as a matrix and steel wire as a fiber were chosen for the composite of this model experiment. Figure 1 shows the results of room temperature tests of an acrylic plate and a steel wire (A-S composite). While the acrylic did not deform plastically, the steel wire did undergo a very limited amount of plastic deformation before fracture.

Experimental Procedures

The fiber composite materials were made by hot-pressing two acrylic plates (Acrylite FF by CYRO Industries) and a steel wire (music wire). The composition of the wire (in wt. %) is C 0.75-0.95, Mn 0.60 max, Si 0.28 max, S 0.030 max, P 0.024 max and Fe balance, and the diameter was about 0.23 mn. For large specimens, a stainless steel rod (4.7 mm in diameter) instead of the music wire was used. The temperature of the hot-press was 155°C ± and the pressure of about 600 psi was slowly applied to the plates and the wire. Then the material was slowly cooled to room temperature. The test pieces were cut using a low speed saw into sizes of $3 \times 10 \times \ell$ mm^3 (where ℓ is the length of the specimen and varies) for small specimens and $9 \times 50 \times 50$ mm^3 for large specimens.

The pull-out tests were performed using an Instron 1125 Machine. Figures 2 and 3 illustrates the specimen and test set-up. The specimen was supported at the shoulders and the wire was held by a pair of stainless steel plates. Cross head speed varied from 0.5 mm/min to 500 mm/min.

Experimental Results

1. "Stick-Slip" and Partial Debonding.

Figure 4(a) shows the plot of load vs. displacement of pull-out tests of an A-S composite with a Si greased wire. The cross-head speed (CHS) was 0.5 mm/min., the specimen length (ℓ) was 20 mm and the length of wire outside the specimen (L) was 50 mm. Initially, the load increased linearly with displacement until a sudden decrease in load occurred with an audible click. During this very brief interval of time, the cross-head continued to move. Thus, after the initial small drop in load the load proceeded to increase again linearly with displacement.This "slip-stick" process was repeated but with the peak load decreasing until the wire was completely pulled out from the specimen. Most of the short specimens and specimens with a greased wire showed this type of load-displacement plot. Similar "stick-slip" sliding was reported in several other composites, for example, in an epoxy-copper composite [2] and in a resin-glass composite [3].

Figure 4(b) shows the other type of load-displacement plot obtained from an A-S composite with an as-received wire tested with the same condition as the previous specimen (CHS = 0.5 mm/min., ℓ = 20 mm and L = 50 mm). Before reaching the maximum peak, several small load drops were observed. Each time this partial "debonding" occurred there was also an audible click. The partially debonded area was distinguished by the difference in visual appearance of the reflection change of the wire from that of the bonded area. The partial debonding started at the loaded end of the fiber and continued throughout the specimen and finally reached the free end of the fiber. After that, the "slip-stick" sliding behavior occurred just as in the previous case. To confirm that the small load drops

correspond to partial debonding, the load was completely released and the sample was then reloaded. The small drops were not observed when the specimen was unloaded and reloaded as shown in Fig. 4(b). Therefore, the small load drops observed before reaching the maximum peak must be caused by the partial debonding between the matrix and the fiber. The debonding of the previous specimen, Fig. 4a, was thought to occur "instantaneously" at the first peak of the load.

2. Effect of Surface Condition of the Wire on Friction Force.

The friction force should be related to the peak in the loading curves. In order to show this, the peak loads were plotted as a function of the displacement of the cross-head for 5 surface conditions in Fig. 5. The magnitude of the peak loads of the specimen with a wire that had been polished with 240 grit emery paper had the largest values, the peak values for specimens with wires that were polished with 400 grit was the second, the peak values for the specimens with the as-received wire was the third and the composites with wire that had an application of apiezon and Si grease prior to fabrication were the smallest. This indicates that the frictional force can be influenced by the surface condition of wire, via polishing and/or the application of a coating of grease. Each curve decreased to zero load at a displacement of 20 mm which was the specimen length, that is, the wire was completely pulled out of the matrix. The reason for the decreasing peak load is mainly due to the decrease in the wire length in the matrix as the wire was pulled out.

3. Simple Analysis of Frictional Force.

The frictional force between the fiber and the matrix has to be a materials constant. In this section, the friction constant is derived from a simple assumption and is subsequently discussed.

Refering to Fig. 6, the followlwing are the notation of variables:

F : the friction constant, the force per unit area required to induce sliding between the fiber and the matrix.

P : the pull-out load.

ℓ : the embedded length of the wire.

$\Delta\ell$: the decrement of the wire length inside the matrix.

D : the diameter of the fiber.

After debonding we assume that the force on the wire inside the matrix is constant (Assumption 1), the force to induce an increment of sliding P', can be given by the product of F and the surface area between the fiber and the matrix, that is:

$$P' = \Pi F \ell D. \tag{1}$$

Sliding occurs when P equals to P' which is at the first peak of the load (not the small peaks of debonding that occurred in the initial loading of the specimen). If we let the load of the first peak be P_1, the friction constant is given as:

$$F = P_1/\Pi \ell D. \tag{2}$$

For the nth increment of sliding, the peak load is P_n and the friction constant is then given as:

$$F = P_n/\Pi\ (\ell - \Delta\ell_n)\ D. \qquad (3)$$

The $\Delta\ell_n$ can be estimated from the load-displacement chart as follows. The $\Delta\ell_n$ is roughly equal to the increment of the wire length outside the matrix when the load is completely released. Therefore, the extrapolation of the load-displacement line to the zero load will give $\Delta\ell_n$ as shown in Fig. 4(a) for n = 8. It is, then, possible to calculate a friction constant, F, for each peak. The results of the calculations are plotted as a function of $\Delta\ell$ in Fig. 7. The frictional constant, F, is relatively constant for the A-S composite with the two greased wires, while those of the other A-S composites with the as-received and polished wires increased with an increase in $\Delta\ell$. The increased values obtained from the A-S composite may be caused by the stress and/or strain distribution in the composite or by the dragging of debris that continues to adher to the wire. Though the friction coefficient, as mentioned earlier, should be a materials constant, the F values increased for the high friction conditions.

4. Effect of Specimen Length on the Friction Force.

The effect of the specimen length, ℓ, on friction force was investigated using A-S composites with as-received wires of different embedded lengths under the conditions of constant CHS (0.5 mm/min.) and constant L (50 mm). Figure 8 shows the friction constant calculated by Eqs.

2 and 3 from the load-displacement charts of pull-out tests of composites with specimen lengths of 7.4, 12.9, 29.6, 32.0 and 33.2 mm, respectively. Even with the different initial specimen length, F values fall along one line. The F value was relatively constant up to $\Delta\ell \approx 8$ mm but then F increased with increasing $\Delta\ell$. However, it appears that the effect of the initial specimen length on F is negligible because all the data falls on one curve.

5. Effect of Pull-Out Test Speed.

5-1. A-S composite with wire.

To ascertain the effect of pull-out speed on the friction constant, F was plotted as a function of $\Delta\ell$ for two "identical" A-S composites tested with CHS's of 0.5 mm/min. and 5 mm/min. in Fig. 9. Slightly smaller values are obtained from the faster test. The change of F with increasing $\Delta\ell$ was very similar for the two CHSs.

The effect of much faster pull-out speed was investigated with an A-S composite. During the test, the load was released after observing 5 to 10 "stick-slip" cycles, the cross-head speed was then changed and the test was resumed. This procedure was repeated with several different cross-head speeds. The resultant load-displacement plot is shown in Fig. 10. The faster the cross-head speed, the smaller the peak amplitude of "stick-slip" process, additionally the "stick-slip" process was not observed with cross-head speed of 500 mm/min.

5.2 A-S Composite with Stainless Steel Rod.

As shown in Fig. 2(b), a large A-S composite was made with a stainless steel rod (4.7 mm in diameter) with both ends of the rod outside the acrylic matrix. The advantage of this configuration for the specimen was the elimination of the effect of $\Delta\ell$. The result of pull-out test with several cross-head speeds is shown in Fig. 11. "Stick-slip" was observed with low cross-head speeds and tended not to be observed with high speeds. The transition between "stick-slip" to no "stick-slip" was determined to be at a cross-head speed of about 50-60 mm/min. for this test.

Discussion

The observation of the coincidence of the movement of the end of the wire with the occurrence of the peak load in the load-displacement graph and the subsequent slip-stick behavior of the load-displacement during the pull-out experiment suggests that we have two different phenomena occurring. We suggest that the initial peak represents the load required for debonding of the steel fiber. The subsequent slip-stick observation must, therefore, be associated with the sliding of the steel fiber in the acrylic matrix. The decrease in the load as the slip-stick phenomenon progresses must be associated with the decrease in contact area as the fiber is pulled from the matrix. The fact that the slip-stick behavior observed in the load-displacement data is dependent upon the surface treatment of the fiber supports this rationalization.

The speed of testing appears to be a critical variable, accentuating or suppressing the load-drops in the load-displacement curves. We believe the pull-out test with the load peaks followed by the load drops is a

consequence of a loading and a relaxation pattern that occurs upon loading the composite in the fiber pull-out configuration. During loading, the steel fiber outside of the acrylic matrix undergoes a larger elastic strain than the steel fiber embedded in the acrylic matrix. Thus, when a small increment of the steel wire is suddenly extracted (pulled out) from the matrix, the load is relaxed in proportion to the difference in elastic strain in the small pulled-out increment and the elastic strain in the rest of the steel fiber. As the cross-head of the testing machine continues to move at a constant velocity, the load-sensor (which is also an elastic member) senses the slight decrease in the average strain with a consequence "instantaneous" drop in the load. Now, as the moving cross-head continues to move, the average elastic strain increases until the load again proceeds to increase. This explanation, to a degree, begs the question of why the pull-out occurs in a discontinuous manner. The answer to this question may reside in invoking the role of static and dynamic friction in the slip-stick loading pattern. Here our explanation is only slightly modified in that the peak load is to be associated with a static frictional force followed by dynamic frictional forces as the fiber slids in the matrix. Again, the load-extension curve must be a consequence of differential elastic strain of the fiber in the embedded and unembedded condition.

The occurrence of the audible "clicks" during the initial load maximum, Fig. 4a, of the specimen were treated so as to decrease the interfacial cohesion, i.e., the fiber was greased prior to fabrication, indicating that debonding occurred at the initial maximum in load. In contrast, the acrylic steel fiber composite without surface treatment. i.e., with better interfacial cohesion, displayed a sequence of load drops in the initial

loading phase, Fig. 4b. Each of these series of peaks were also accompanied by audible clicks. However, once debonding had occurred at the first large maximum in the load, the subsequent load maximum were not accompanied by audible clicks. In addition, the process of debonding in the composite with good interfacial cohesion was visible as reflection at the interface that progressed along the fiber during the series of audible clicks and peaks in the initial loading phase.

Based upon this argument for sliding, an expression was formulated for the frictional constant that resisted the movement of the steel fiber in the composite. The frictional constant (the frictional force per unit area) was clearly shown to depend upon the surface treatment of the fiber but was not constant except in the case where interfacial cohension was very low, the greased fibers. The increase in the frictional force with a decrease in the length of the embedded fiber may reside with either an internal stress state, the accumulation of debris as the fiber moves or possibly there may be a slight mechanical effect on the very end of the wire that would become increasingly important as the length of the embedded fiber decreased. The frictional constant was also found to be independent of the initial length of the composite specimen, in that the friction constant for specimens with length from 7.4 to 33.2 mm all fall in the same curve with respect to the decrease in length of the embedded fiber. Here again, however, the frictional constant increase as the length of the embedded fiber decreased, an exception may have been the very short, 7.4 mm, specimen.

The inverse dependence of the frictional constant upon the speed of testing appears to suggest that the segmenting of the frictional behavior into static and dynamic behavior may be correct. The slower speed being

associated with greater static component than the higher speed. An alternative hypothesis would be to suggest an adiabatic effect on the matrix at the interface.

Finally, the demonstration that the load drops in the stick-slip phenomenon were obscured by sufficiently high rates of loading supported the role of relaxation of the load sensing element during the load drops in the pull-out tests. This was observed on two different specimen geometries and suggest that slip-stick observations may occur in other composites when loading conditions are favorable.

Conclusions

While this research is still in progress, the following conclusions seem justified at this time.

1. Debonding in A-S composites with low interfacial coherency is accompanied by an audible click and a drop in the paak load.
2. An A-S comopsite with good interfacial coherency appears to undergo debonding in a sequence of stages.
3. The interfacial coherency is easily influenced in A-S composites by either mechanical or chemical treatment.
4. The role of friction in pull-out tests seems to require the utilization of both a static and a dynamic parameter when dealing with A-S composites.
5. The slip-stick phenomenon in A-S composites can be obscured at sufficiently high rates of testing.

References

1. D. B. Marshall and A. G. Evans, "Failure Mechanisms in Ceramic-Fiber/Ceramic-Matrix Composites", Jnl. Am. Cer. Soc. 68 (1985), 225.

2. R. F. Cook, M. D. Thouless, D. R. Clarke, and M. C. Kroll, "Stick-Slip During Fiber Pull-Out", Scripta Metull. 23 (1989), 1725.

3. "Bond Studies in Glass Reinforced Plastics", Progress Report MCA-MIT Plastics Research Project, Plastics Research Laboratory, MIT, Oct. 1, 1957.

Figure Captions

Fig. 1 Tensile stress-strain curves of acrylic sheet (l = 25.0, w = 12.5 and t = 2.9 mm) and steel wire (ℓ = 8.3 and d = .228 mm) with CHS = 0.5 mm/min. at room temperature (22°C). Young's modulus of the acrylic and steel wire were 2.2 and 197 GPa respectively. $\sigma_{p\ell}$ = 2.76 GPa for the steel wire.

Fig. 2 Specimen size and configuration-schematic.

Fig. 3 Pull-out test configuration.

Fig. 4 Load-displacement plots of pull-out tests of a) A-S composite with a greased wire and b) A-S composite with an as-received wire.

Fig. 5 Peak load-displacement plots of pull-out tests of A-S composites with: a) ■ = wire polished with 240 grid; b) □ = wire polished with 400 grid; c) Δ = as-received wire; d) ● = apiezon vacuum seal greased wire: and e) ○ = Si vacuum greased wire.

Fig. 6 The definitions of the variables used to determine Friction Constant.

Fig. 7 Plots of friction constant-decrement of wire length inside the matrix for A-S composites with: a) wire polished with 240 grid; b) wire polished with 400 grid; c) as-received wire; d) vacuum seal greased wire; and e) Si greased wire.

Fig. 8 Plots of friction constant-decrement of wire length inside the matrix for A-S composites with different composite specimen lengths.

Fig. 9 Plots of friction constant-decrement of wire length inside the matrix for A-S composites with different cross-head speeds: a) 0.5 mm/min; and b) 5 mm/min.

Fig. 10 Load-displacement plot of a pull-out test of an A-S composite with different cross-head speeds.

Fig. 11 Load-displacement plot of a pull-out test of a 4.7 mm diameter stainless steel rod-acrylic composite with different cross-head speeds.

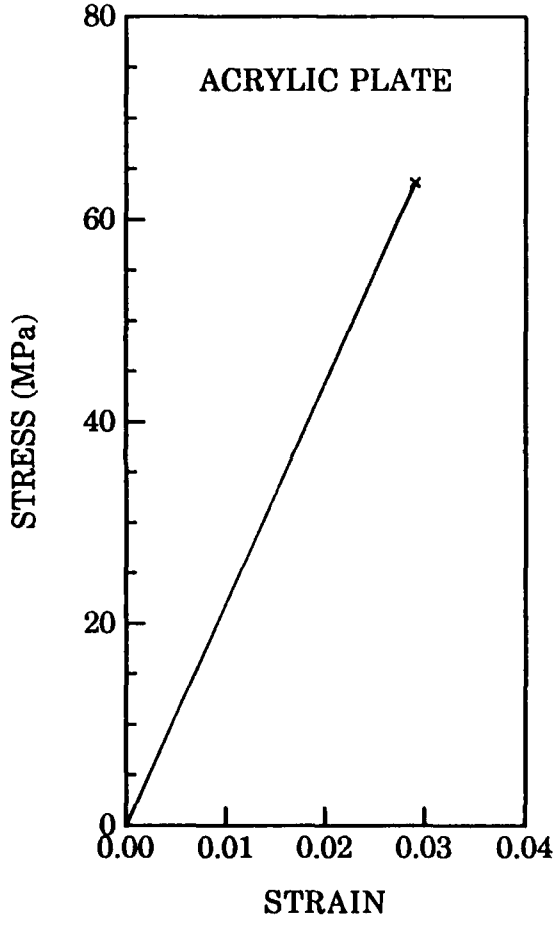
ACRYLIC PLATE
STRESS (MPa)
80
60
40
20
0
0.00
0.01
0.02
0.03
0.04
STRAIN

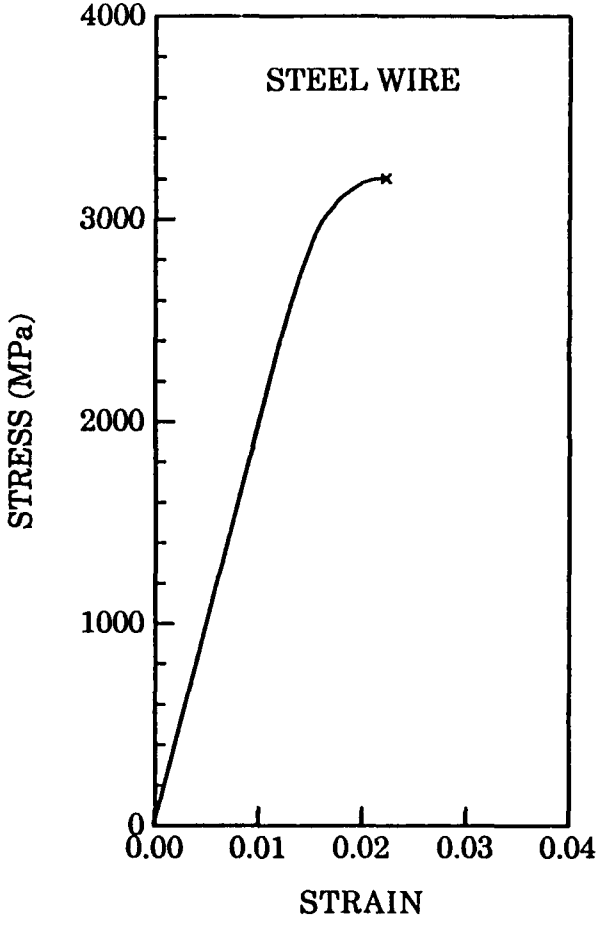
STEEL WIRE
STRESS (MPa)
4000
3000
2000
1000
0
0.00
0.01
0.02
0.03
0.04
STRAIN

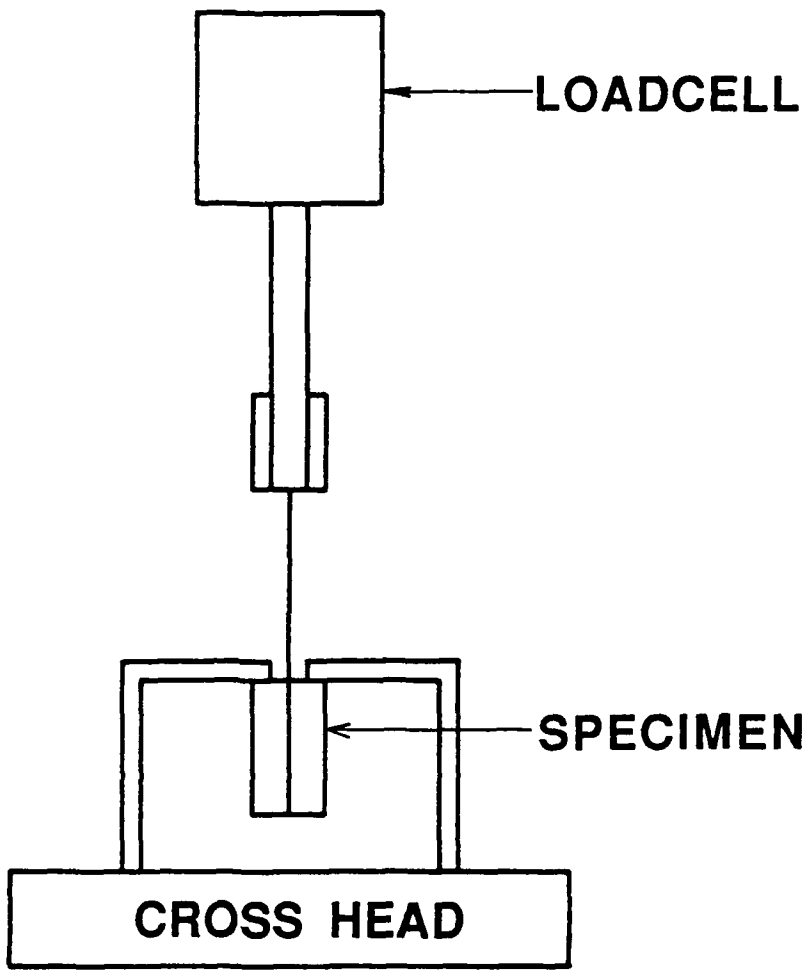
LOADCELL
SPECIMEN
CROSS HEAD

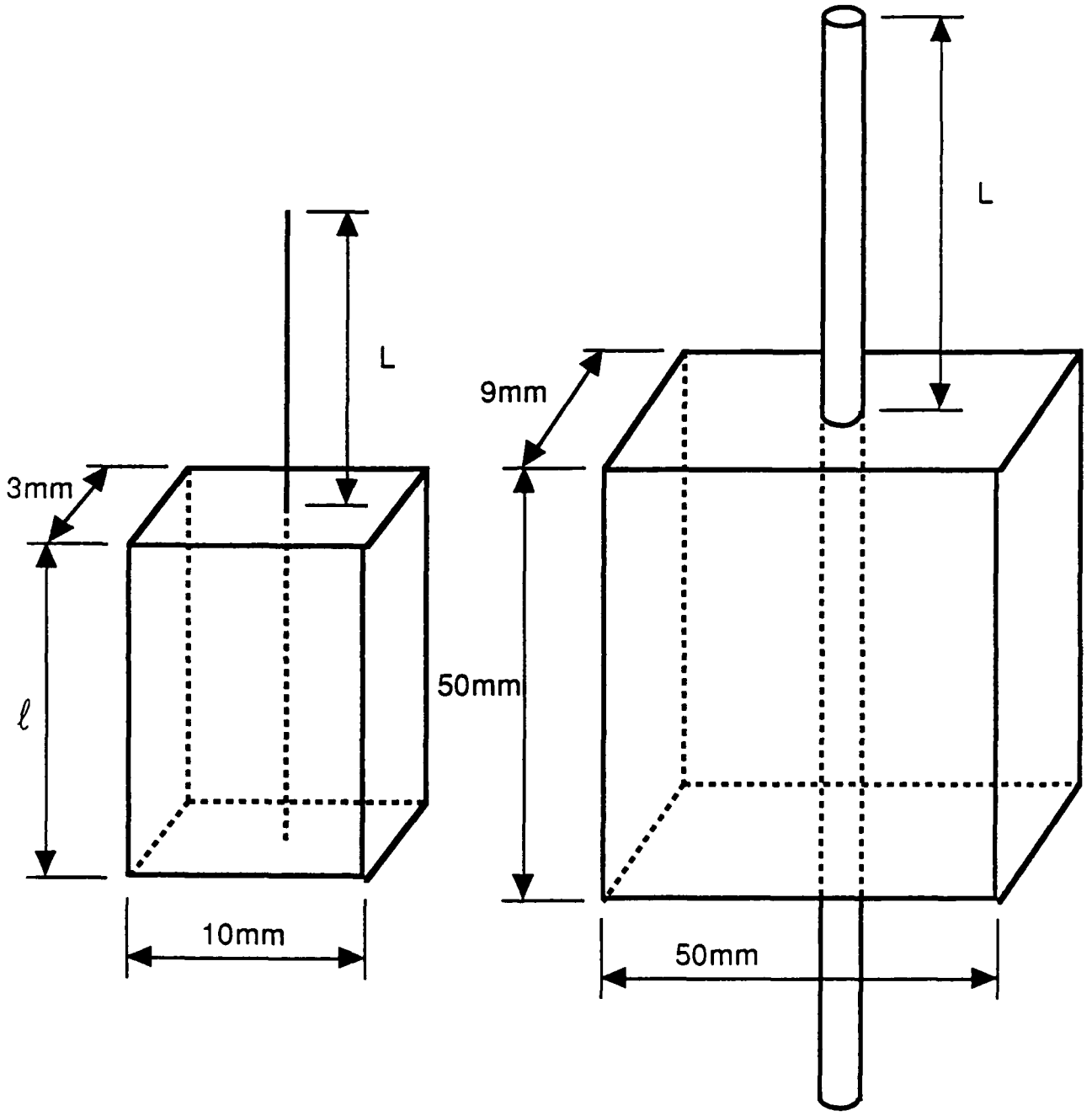

Fig 3

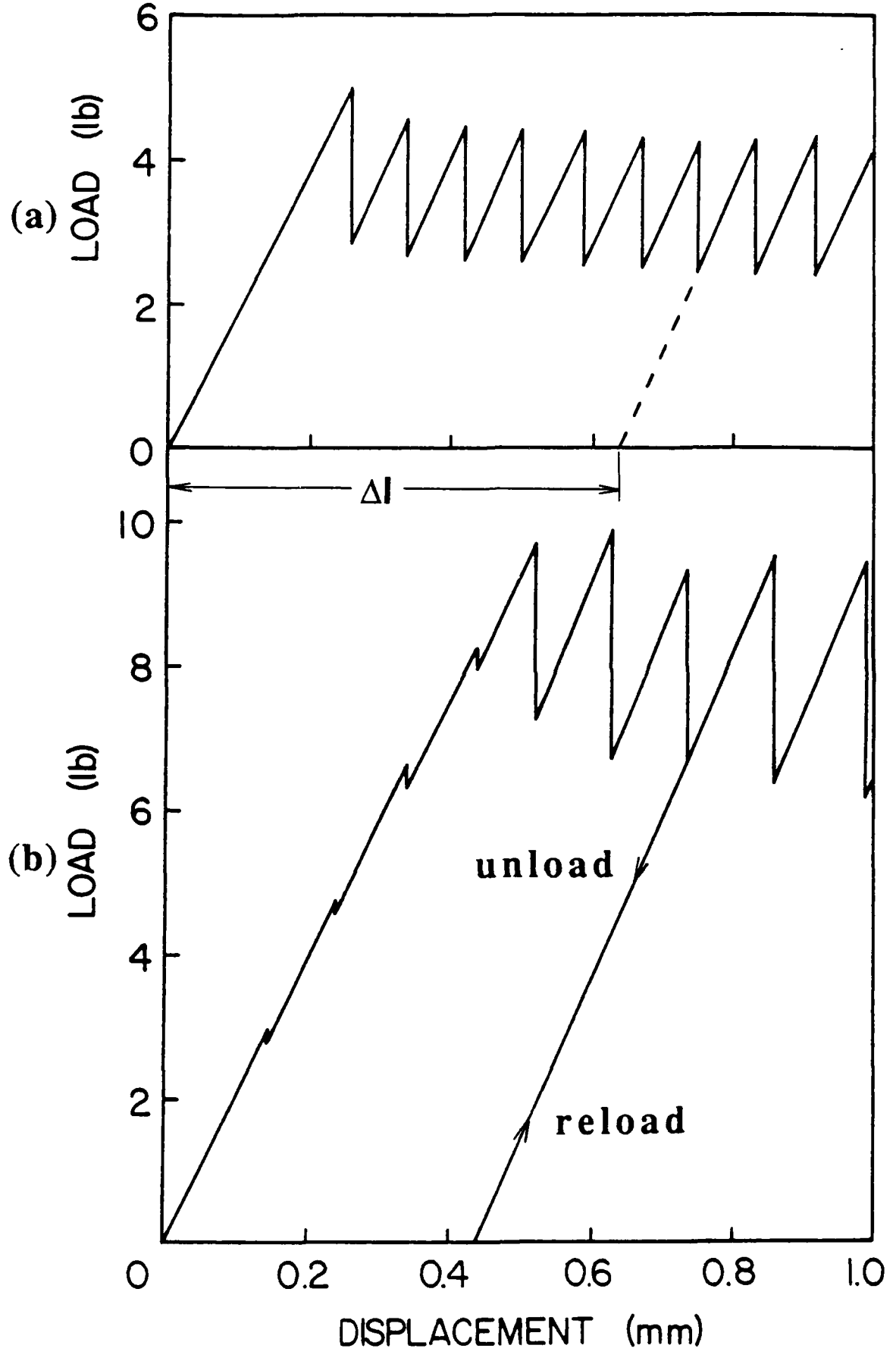
(a)
LOAD (lb)
6
4
2
0
Δl
(b)
LOAD (lb)
10
8
6
4
2
unload
reload
0
0.2
0.4
0.6
0.8
1.0
DISPLACEMENT (mm)

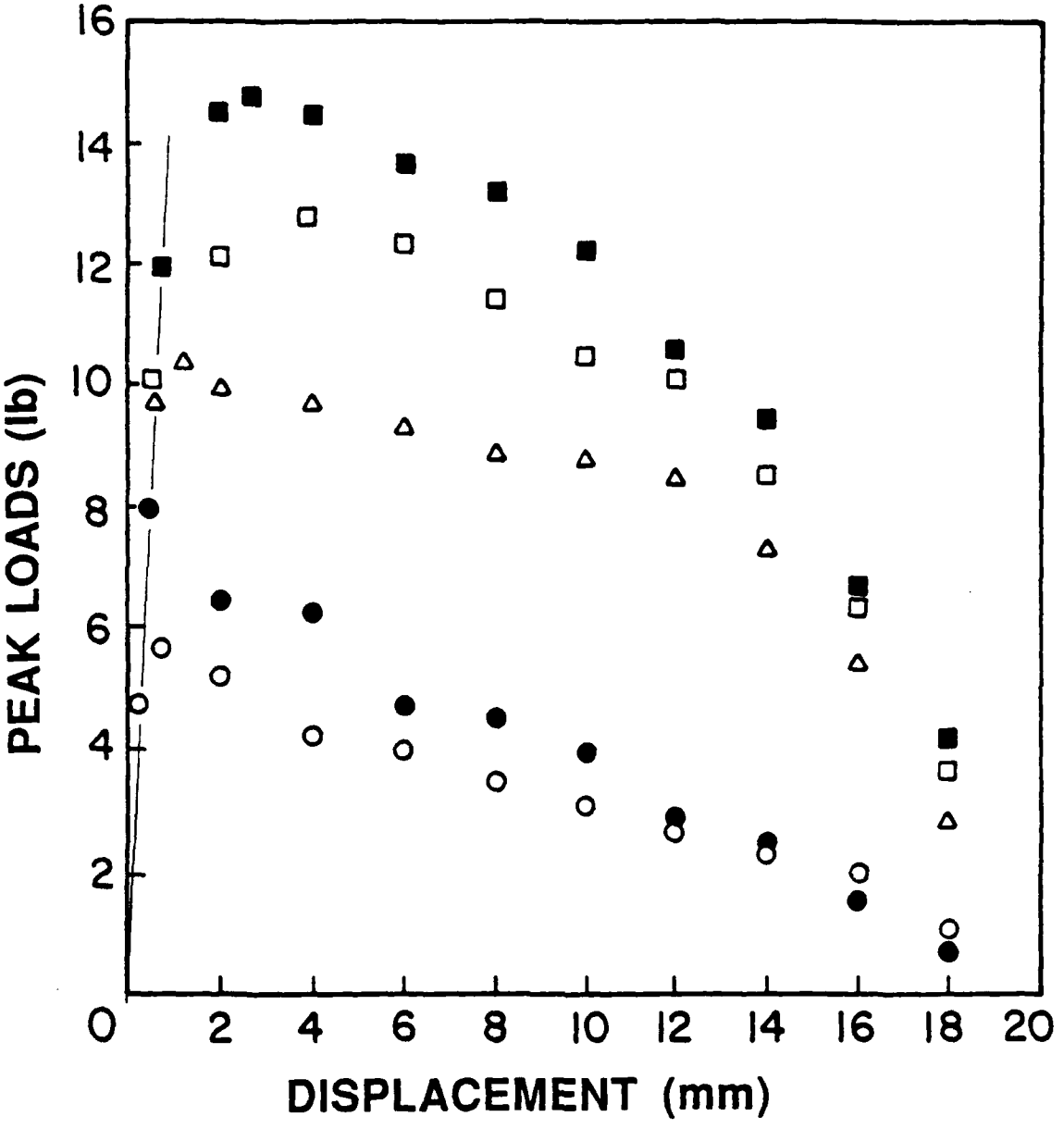
PEAK LOADS (lb)
16
14
12
10
8
6
4
2
0
2
4
6
8
10
12
14
16
18
20
DISPLACEMENT (mm)

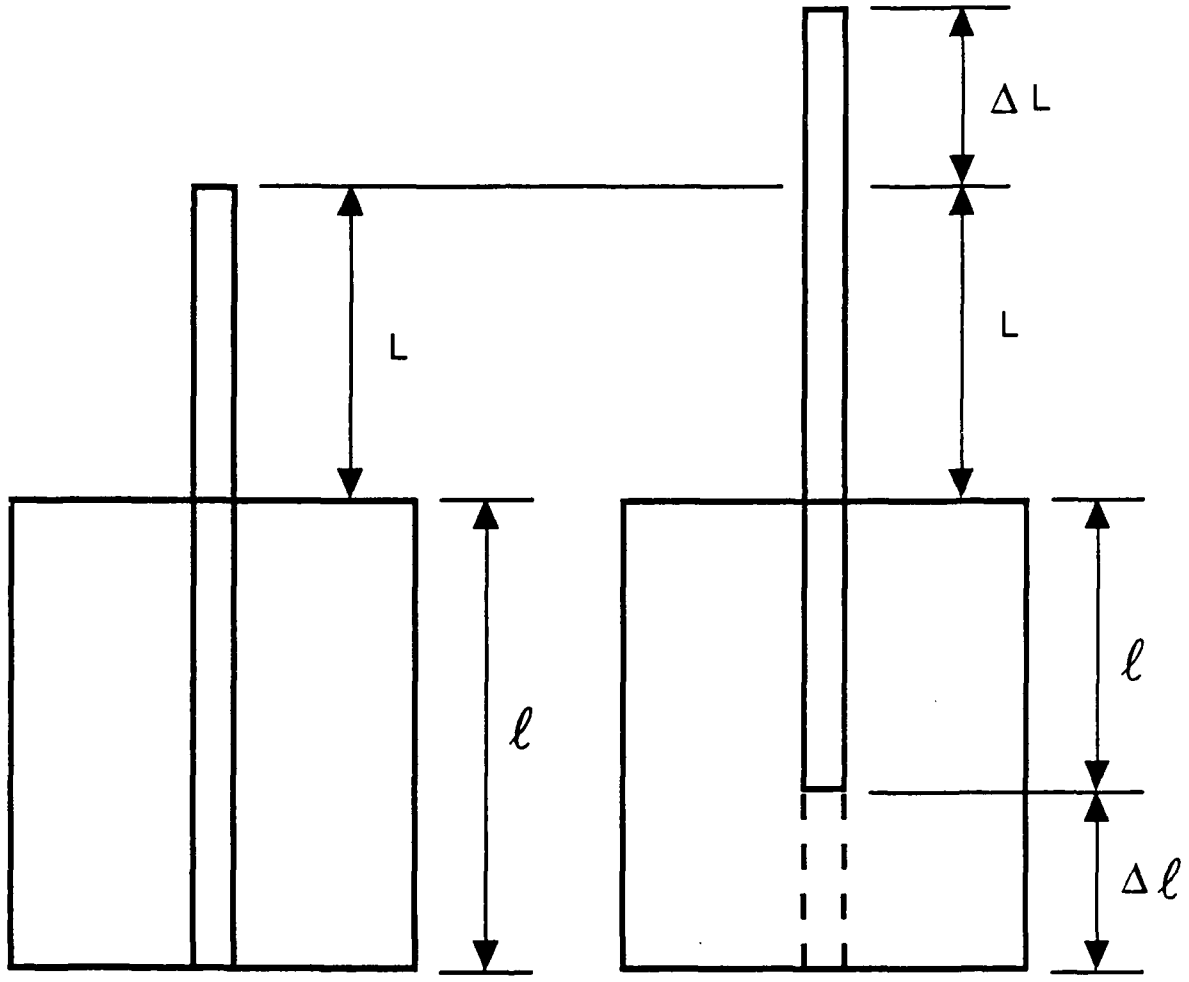

Fig 6

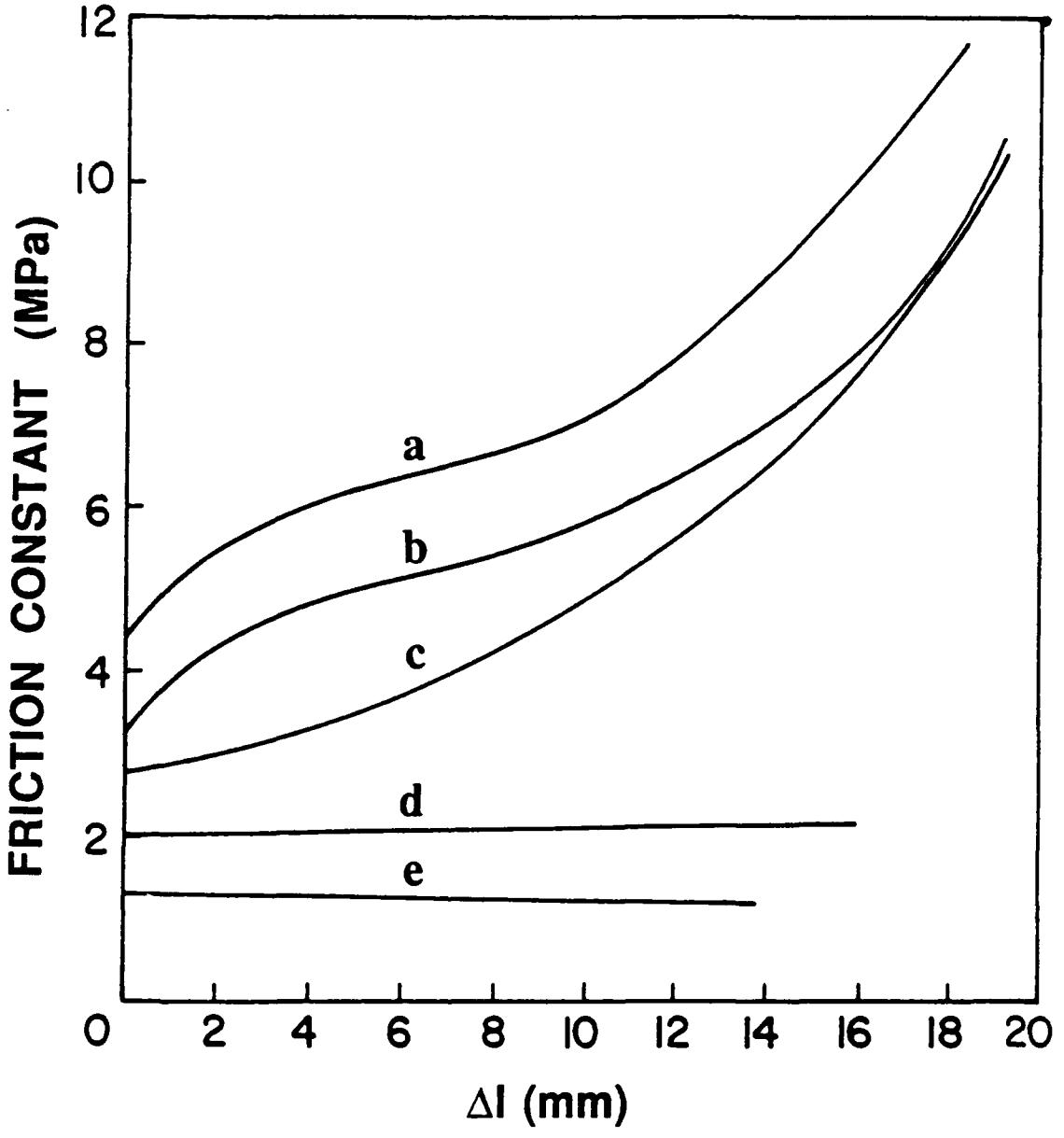
FRICTION CONSTANT (MPa)
12
10
8
6
4
2
0
2
4
6
8
10
12
14
16
18
20
ΔI (mm)
a
b
c
d
e

Fig

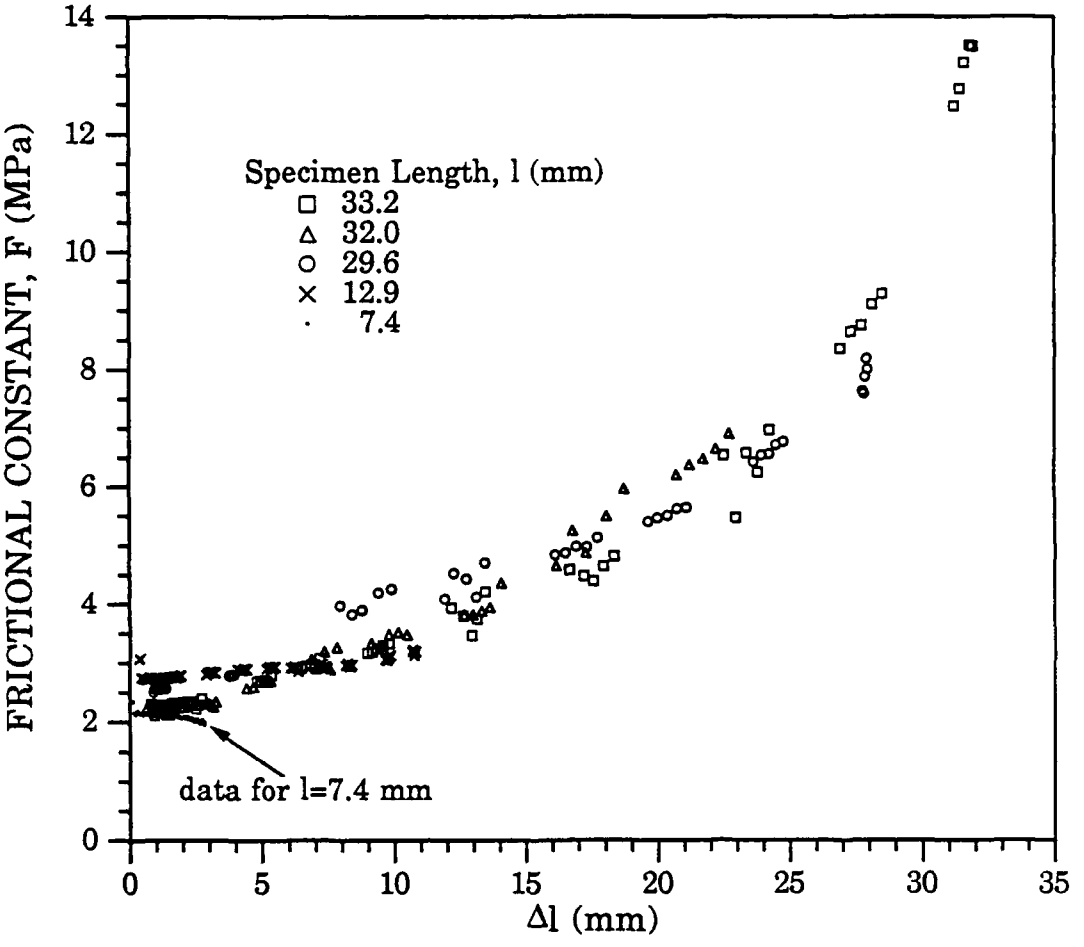
FRICTIONAL CONSTANT, F (MPa)
Δl (mm)
Specimen Length, l (mm)
33.2
32.0
29.6
12.9
7.4
data for l=7.4 mm
0
2
4
6
8
10
12
14
0
5
10
15
20
25
30
35

Fig 2

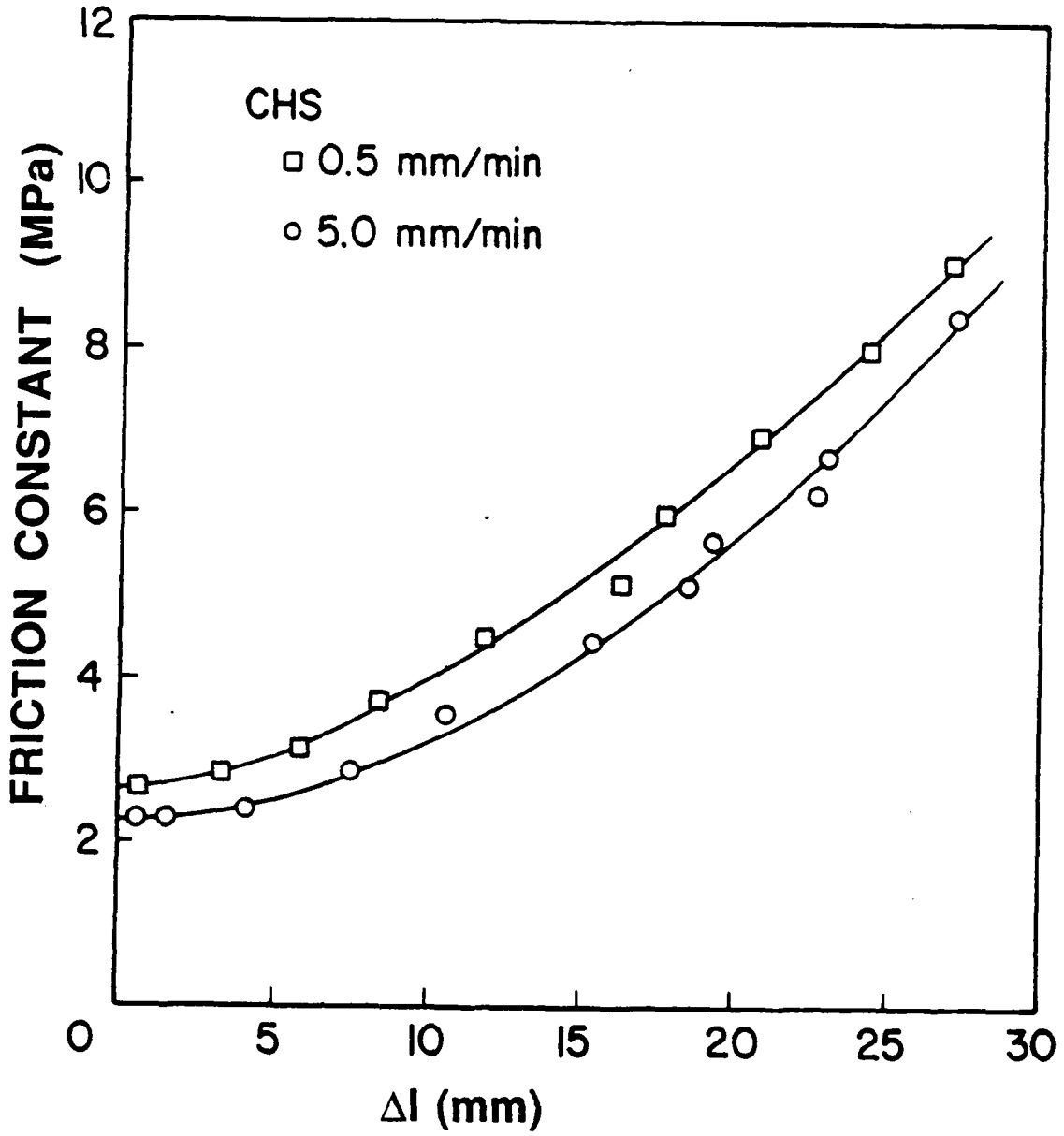
CHS
0.5 mm/min
5.0 mm/min
FRICTION CONSTANT (MPa)
ΔI (mm)
0
2
4
6
8
10
12
5
10
15
20
25
30

Fig 9

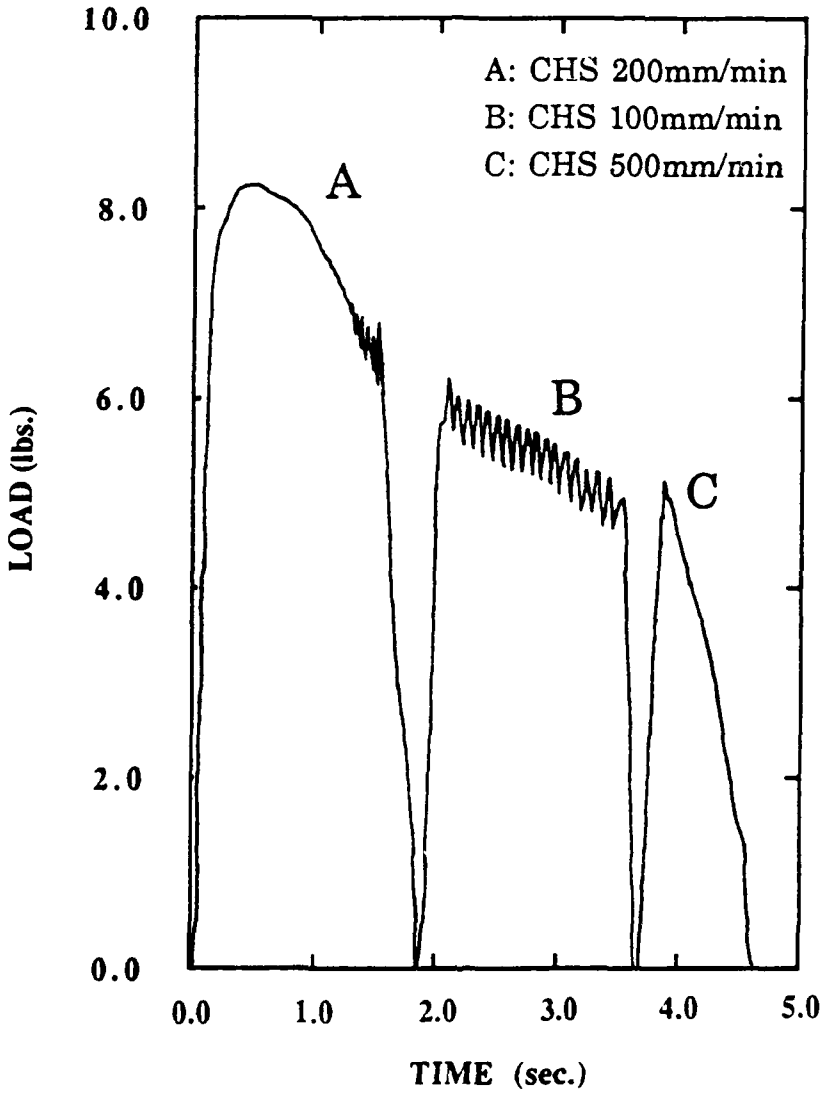
10.0
8.0
6.0
4.0
2.0
0.0
LOAD (lbs.)
A: CHS 200mm/min
B: CHS 100mm/min
C: CHS 500mm/min
A
B
C
0.0
1.0
2.0
3.0
4.0
5.0
TIME (sec.)

Fig 1c

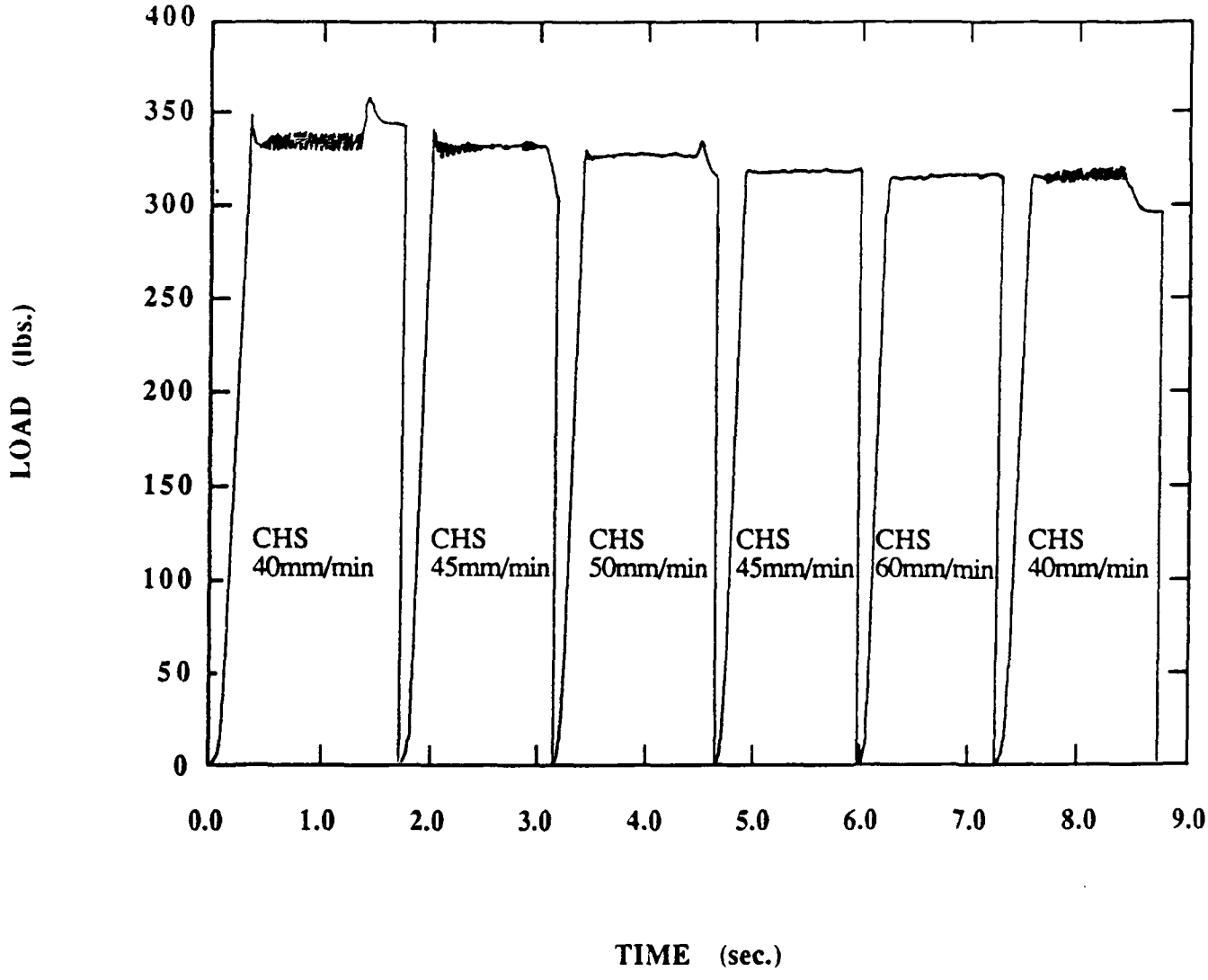
400
350
300
250
200
150
100
50
0
LOAD (lbs.)
CHS
40mm/min
CHS
45mm/min
CHS
50mm/min
CHS
45mm/min
CHS
60mm/min
CHS
40mm/min
0.0
1.0
2.0
3.0
4.0
5.0
6.0
7.0
8.0
9.0
TIME (sec.)

Fig 2

SINGLE FIBER TESTS: CERAMIC MATRIX - CERAMIC FIBER COMPOSITES

D. R. MUMM AND K. T. FABER

INTRODUCTION:

The high toughness exhibited by recently developed fiber-reinforced ceramic composites has been attributed to a fiber bridging, debonding and pullout mechanism. This toughening mechanism has been studied extensively experimentally and analytically, with generally all of the models indicating that fiber debonding is a prerequisite for pullout and may itself make an important contribution to the toughness. Despite its relative importance to the toughening of all-brittle materials, there has been no direct experimental verification of the debonding behavior during fiber pullout.

It is the initial objective of this research project to study the *in-situ* debonding behavior during fiber pullout in a ceramic composite by utilizing a photoelastic technique. It is anticipated that while testing a model single-fiber pullout specimen, the photoelastic apparatus will allow direct observation of the dynamic debond crack propagation. As the debonding is occuring during a pullout test, where the fiber is pulled in a standard tensile testing apparatus, the load-displacement data is simultaneously obtained and may be directly correlated to the observed behavior. In addition, the photoelastic analysis should indicate qualitatively the changes in the matrix stress distribution which occur during fiber debonding and pullout. This testing procedure should resolve the ambiguities in interpreting the load-displacement curves of single-fiber pullout tests [see curve (b) in Figure 1].

BACKGROUND:

Photoelasticity:

The photoelastic analysis relies on the stress birefringence properties of glass. When glass is stressed, it becomes optically anisotropic; the indices of refraction change. These changes are directly proportional to the stresses and follow the relationships below:

$$n_1 - n_0 = C_1 \sigma_1 + C_2 \sigma_2$$
$$n_2 - n_0 = C_1 \sigma_2 + C_2 \sigma_1$$

$$n_2 - n_1 = C (\sigma_1 - \sigma_2)$$

$$C = C_2 - C_1$$

where n_1, n_2 are the indices of refraction in the principal stress directions, n_0 is the index of refraction in the unstressed, optically isotropic material, σ_1, σ_2 are the principal stresses in the plane normal to the direction of the light propagation, C_1, C_2 are constants of proportionality, and C is the relative stress-optical coefficient for the material and is a material property.

The governing stress-optic law is:

$$\sigma_1 - \sigma_2 = \frac{N f_\sigma}{h}$$

where h is the thickness of the sample under stress, N is the fringe order and is the relative retardation of the light in terms of one complete wavelength, and f_σ is the material fringe value and is defined as:

$$f_\sigma = \frac{\lambda}{C}$$

where λ is the wavelength of the light.

The implications of the stress-optic law are that [1] the stress in the glass is determined by the fringe order (the value of N), [2] points of stress concentration are shown as regions of closely spaced fringes, and [3] a moving crack front can be followed by the movement of the fringes. In front of a debond crack, the matrix stress field is the superposition of the residual stresses from thermal mismatch and the stresses due to load transfer from the fiber to the matrix. Behind the debond crack tip, the matrix stress field near the fiber consists primarily of the residual clamping stresses. In cases where the interface is under residual compression and the thermal expansion mismatch is large, the interface behind the crack tip may still transfer a significant portion of the load applied to the fiber and the matrix stress field will still be a superposition of the two effects. The debond crack tip is a region of stress concentration and is denoted in this setup by a relative concentration of fringes.

EXPERIMENTAL:

Sample Preparation:

The samples to be used in this analysis are to consist of ceramic rods embedded in a transparent glass matrix. The use of large diameter ceramic rods to model the fibers and glass to model the brittle matrix in a ceramic composite is due to the requirements posed by the techniques of photoelastic analysis. With reference to the above stress optic law, it can be seen that since the stress-optical sensitivity of glass is relatively low (small

relative stress optical coefficient) to get an observable fringe order N, the thickness h must be sufficiently large. The sample geometry is such that both ends of the ceramic protrude from the glass block, with collars epoxied to the ends of the rod to facilitate the application of load [Figure 2]. The front and back faces of the glass matrix are to be ground flat and parallel and polished, as this is necessary for the photoelastic analysis.

A conventional pullout sample will not work for this analysis for the reasons mentioned above. In a conventional pullout specimen, where the fiber diameters are < 140μm, the load transfered from the fiber to the matrix prior to either fiber fracture or debonding and pullout is insufficient to produce observable photoelastic fringes. The slow axis of the polarized light is not sufficiently retarded relative to the fast axis such that any destructive interference occurs. In addition, it can be seen from the stress-optic law that the retardation is proportional to the thickness of the sample under stress. With the small diameter of the fibers, the thickness h is small and the retardation of the light is minimized.

The rod will either be notched or through cut before it is embedded in the glass such that after load is applied, the resulting two sections of the rod have different embedded lengths. This will (most likely) ensure that the top section of the rod will pull out of the matrix, leaving the interface of the bottom section intact.

Preliminary samples will consist of mullite rods (α = 4.5 x10^{-6} °C^{-1}) embedded in a matrix of Corning code 7740 (Pyrex) glass (α = 3.5 x10^{-6} °C^{-1}). Later samples may use different compositions of glass and ceramic rods to investigate the effect of the thermal expansion mismatch on the observed debonding behavior. Goettler and Faber [Comp. Sci. Tech., 37 (1989) 129-147] have used a soda-borosilicate glass to investigate the effect of the thermal expansion mismatch on the interfacial shear strengths. The thermal expansion coefficient of this glass varies linearly with Na_2O weight percent from approximately 3 x10^{-6} (°C^{-1}) to 9 x10^{-6} (°C^{-1}).

To get the weak interface necessary for debonding rather than "fiber" failure, the ceramic rods will be carbon coated using a standard SEM carbon sputter apparatus. By varying the thickness of the carbon coating, the strength of the chemical bond between the rod and the matrix can be varied. In addition, the thickness of the coating will have an effect on the residual clamping stress, as the coating has a higher compliance than the ceramic rod and will releive some of the stress due to thermal mismatch.

The actual sample fabrication will utilize a graphite mold. After the rod is secured in the mold, glass in the form of fine powder is to be poured into the mold. Inside an inert atmosphere furnace retort the assembly will then be heated to temperatures exceeding 1000°C to allow the glass to consolidate and flow. The assembly is then to be cooled slowly to the annealing temperature and held to allow any anomalous stresses within the glass to relax. Furnace cooling to room temperature will then follow. There is some

question as to whether or not the powder can be consolidated into a transparent, pore free material via this process. If this method fails, the glass can be melted at temperatures exceeding 1500°C and cast into plates which can then be fused together around the rod following the above procedures.

Preliminary Results:

A number of attempts have been made to make a model pullout specimen for this analysis. However, none has produced a successful sample. Initially, specimens were prepared by fusing together glass slides (standard microscope slides) which were placed around an alumina rod. The glass was heated on a BN-coated porcelain plate and allowed to flow. Due to a large thermal mismatch between the components, the matrix, which was put in tension, cracked severely. In addition, problems included the fact that the rod was not parallel to the front and back faces of the glass matrix, and the rod had flowed such that the thickness was reduced too much. This made it apparent that [1] some sort of mold of near final sample dimensions was needed, [2] the thermal expansion coefficients of the components had to be much better matched, and [3] the rod must be supported within the mold so that it remains parallel to the sample faces.

Using Pyrex glass and mullite rods, specimens were fabricated by casting melted glass (1500°C) into a graphite fabric lined mold. The rod was severely thermal shocked, even though it was preheated to a temperature far above the annealing point of the glass.

FUTURE WORK:

Subsequent samples for testing will be made using Nicalon SiC fibers and Nextel alumino-borosilicate fibers. The knowledge of debonding and pullout gained from single fiber experiments will be extended to single fibers in crystalline ceramic matrices, and finally, to full scale composites.

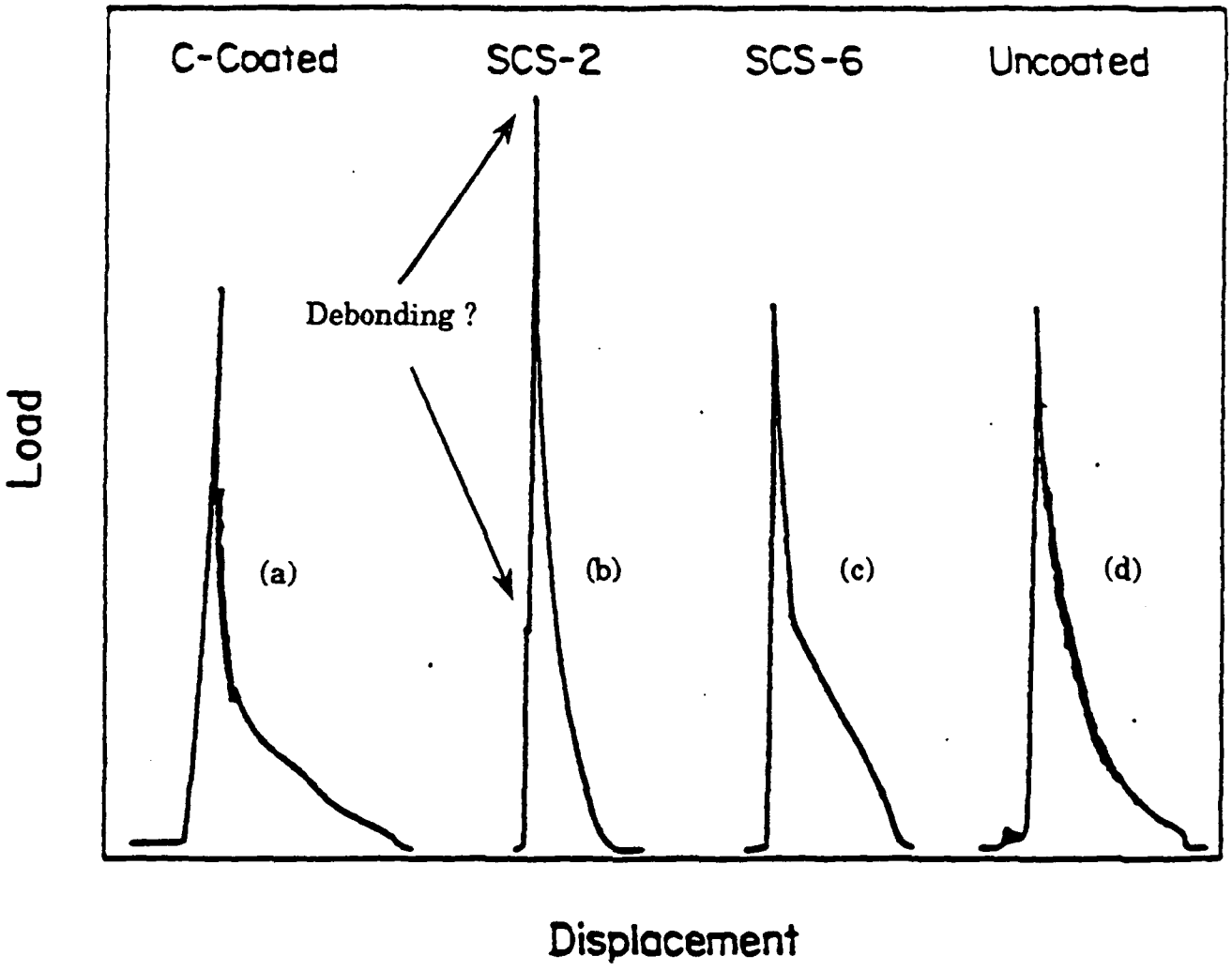

Figure 1 Pullout curves obtained for SiC fibers from glasses of similar thermal expansion (from R. W. Goettler and K. T. Faber, to appear in Composite Science and Technology, December 1989).

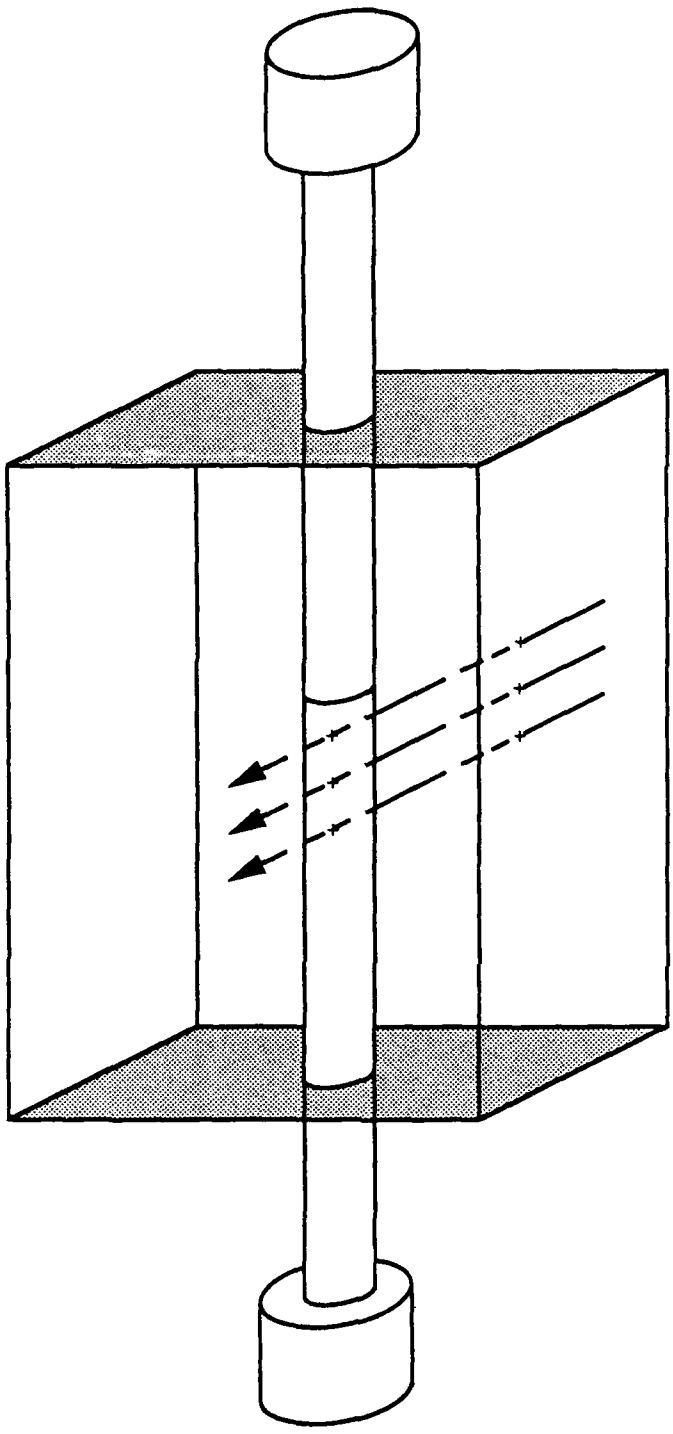

Figure 2 Sample geometry showing polarized light path.